

Spike-based local synaptic plasticity: A survey of computational models and neuromorphic circuits

Lyes Khacef¹, Philipp Klein¹, Matteo Cartiglia²,
Arianna Rubino², Giacomo Indiveri², Elisabetta Chicca¹

¹ Bio-Inspired Circuits and Systems (BICS) Lab., Zernike Institute for Advanced Materials, Groningen Cognitive Systems and Materials Center, University of Groningen, Netherlands.

² Institute of Neuroinformatics, University of Zurich and ETH Zurich, Switzerland.

E-mail: l.khacef@rug.nl

September 2022

Abstract. Understanding how biological neural networks carry out learning using spike-based local plasticity mechanisms can lead to the development of powerful, energy-efficient, and adaptive neuromorphic processing systems. A large number of spike-based learning models have recently been proposed following different approaches. However, it is difficult to assess if and how they could be mapped onto neuromorphic hardware, and to compare their features and ease of implementation. To this end, in this survey, we provide a comprehensive overview of representative brain-inspired synaptic plasticity models and mixed-signal CMOS neuromorphic circuits within a unified framework. We review historical, bottom-up, and top-down approaches to modeling synaptic plasticity, and we identify computational primitives that can support low-latency and low-power hardware implementations of spike-based learning rules. We provide a common definition of a locality principle based on pre- and post-synaptic neuron information, which we propose as a fundamental requirement for physical implementations of synaptic plasticity. Based on this principle, we compare the properties of these models within the same framework, and describe the mixed-signal electronic circuits that implement their computing primitives, pointing out how these building blocks enable efficient on-chip and online learning in neuromorphic processing systems.

Keywords: *brain-inspired computing, neuromorphic CMOS circuits, spiking neural networks, local synaptic plasticity, online learning.*

1. Introduction

The ability of biological systems to learn and adapt to their environment is key for survival. This learning ability is expressed mainly as the change in strength of the synapses that connect neurons, to adapt the structure and function of the underlying network. The neural substrate of this ability has been studied and modeled intensively, and many brain-inspired learning rules have been proposed (McNaughton et al. 1978, Gerstner et al. 1993, Stuart & Sakmann 1994, Markram et al. 1995). The vast majority, if not all, of these biologically plausible learning models rely on local plasticity mechanisms, where locality is a fundamental computational principle,

naturally emerging from the physical constraints of the system. The principle of locality in synaptic plasticity presupposes that all the information a synapse needs to update its state (e.g., its synaptic weight) is directly accessible in space and immediately accessible in time. This information is based on the activity of the pre- and post-synaptic neurons to which the synapse is connected, but not on the activity of other neurons to which the synapse is not physically connected (Zenke & Neftci 2021).

From a biological perspective, locality is a key paradigm of cortical plasticity that supports self-organization, which in turn enables the emergence of consistent representations of the world (Varela et al. 1991). From the hardware development perspective, the principle of locality is a key paradigm for the design of spike-based plasticity circuits integrated in embedded systems, in order to enable them to learn online, efficiently and without supervision. This is particularly important in recent times, as the rapid growth of wearable and specialized autonomous sensory-processing devices brings new challenges in analysis and classification of sensory signals and streamed data at the edge. Consequently, there is an increasing need for online learning circuits that have low latency, are low power, and do not need to be trained in a supervised way with large labeled data-sets. As standard von Neumann computing architectures have separated processing and memory elements, they are not well suited for simulating parallel neural networks, they are incompatible with the locality principle, and they require a large amount of power compared to in-memory computing architectures. In contrast, neuromorphic architectures typically comprise parallel and distributed arrays of synapses and neurons that can perform computation using only local variables, and can achieve extremely low-energy consumption figures. In particular, analog neuromorphic circuits operate the transistors in the weak inversion regime using extremely low currents (ranging from pico-Amperes to micro-Amperes), small voltages (in the range of a few hundreds of milli-Volts), and use the physics of their devices to directly emulate neural dynamics (Mead 1990). The spike-based learning circuits implemented in these architectures can exploit the precise timing of spikes and consequently take advantage of the high temporal resolutions of event-based sensors. Furthermore, the sparse nature of the spike patterns produced by neuromorphic sensors and processors can give these devices even higher gains in terms of energy efficiency.

Given the requirements to implement learning mechanisms using limited resources and local signals, animal brains still remain one of our best sources of inspiration, as they have evolved to solve similar problems under similar constraints, adapting to changes in the environment and improving their survival chances (Hofman 2015). Bottom-up, brain-inspired approaches to implement learning with local plasticity can be very challenging for solving real-world problems, because of the lack of a clear methodology for choosing specific plasticity rules, and the inability to perform global function optimization (as in gradient back-propagation) (Eshraghian et al. 2021). However, these approaches have the potential to support massively parallel and distributed computations and can be used for adaptive online systems at a minimum energy cost (Neftci et al. 2019). Recent work has explored the potential of brain-inspired self-organizing neural networks with local plasticity mechanisms for spatio-temporal feature extraction (Bichler et al. 2012), unsupervised learning (Diehl & Cook 2015, Iyer & Basu 2017, Hazan et al. 2018, Kheradpisheh et al. 2018, Khacef et al. 2020b), multi-modal association (Khacef et al. 2020a, Rathi & Roy 2021), adaptive control (DeWolf et al. 2020), and sensory-motor interaction (Lallec &

Dominey 2013, Zahra & Navarro-Alarcon 2019).

Some of the recently proposed models of plasticity have introduced the notion of a “third factor”, in addition to the two factors used in learning rules, derived from local information present at the pre- and post-synaptic site. In these three-factor learning rules, the local variables are used to determine the potential change in the weight (e.g., by using a local eligibility trace), but the change in the weight is applied only when the additional third factor is presented. This third factor represents a feedback signal (e.g., reward, punishment, or novelty) which could be implemented in the brain for example by diffusion of neuromodulators, such as dopamine (Łukasz Kuśmierz et al. 2017, Gerstner et al. 2018). While this feedback signal is locally accessible to the synapse, it is not produced directly at the pre- or post-synaptic site. Therefore, these three-factor learning rules violate the principle of locality that we consider in this review.

In the next section, we provide an overview of synaptic plasticity from a historical, experimental, and theoretical perspective, with a focus on compatibility with physical emulation on Complementary Metal-Oxide-Semiconductor (CMOS) systems. We then present a selection of representative spike-based synaptic plasticity models that adhere to the principle of locality and that can therefore be implemented in neuromorphic hardware. We then present analog CMOS circuits that implement the basic mechanisms present in the rules discussed. As different implementations have different characteristics that impact the type and number of elements that use local signals, for each target implementation, we assess the principle of locality taking into account the circuits’ physical constraints. We conclude proposing steps to reach a unified plasticity framework and presenting the challenges that still remain open in the field.

2. Synaptic plasticity overview

2.1. A brief history of plasticity

The quest for understanding learning in human beings is a very old one, as the process of acquiring new skills and knowledge was already a subject of debate among philosophers back in Ancient Greece where Aristotle introduced the notion of the brain as a blank state (or *tabula rasa*) at birth that was then developed through education (Markram et al. 2011). It was in contrast to the idea of Plato, his teacher, who believed the brain was pre-formed in the “heavens” then sent to earth to join the body. In modern times, the question of nature versus nurture is still being debated, with the view that we are born without preconceptions and our brain is molded by experience proposed by modern philosophers such as Locke (1689), and the studies that emphasize the importance of pre-defined structure in the nervous system and in neural networks, to guide and facilitate the learning process (Binas et al. 2015, Hawkins et al. 2017, Suárez et al. 2021).

In the later half of the nineteenth century, learning and memory were linked for the first time to “junctions between cells” by Bain (1873), even before the discovery of the synapse. In 1890, the psychologist William James postulated a mechanism for associative learning in the brain: “When two elementary brain-processes have been active together or in immediate succession, one of them, on reoccurring, tends to propagate its excitement into the other” (James 1890). In the same period, neuroanatomists discovered the two main components of the brain:

neurons and synapses. They postulated that the brain is composed of separate neurons (Waldeyer 1891), and that long-term memory does requires the growth of new connections between existing neurons (Ramón y Cajal 1894). These connections became known then as “synapses” (Sherrington 1897). At the end of the nineteenth century, synapses were already thought to control and change the flow of information in the brain, thus being the substrate of learning and memory (Markram et al. 2011).

The first half of the twentieth century confirmed this hypothesis by various studies on the chemical synapses and the direction of information flow among neurons, going from the pre-synaptic axons to the post-synaptic dendrites. Neural processing was associated to the integration of synaptic inputs in the soma, and the emission of an output spike once a certain threshold was reached, propagating along the axon. Donald Hebb combined earlier ideas and recent discoveries on learning and memory in his book “The Organization of Behavior”. Similarly to the ideas of James 60 years earlier, Hebb published, in 1949, his formal postulates for the neural mechanisms of learning and memory: “When an axon of cell A is near enough to excite a cell B and repeatedly or persistently takes part in firing it, some growth process or metabolic change takes place in one or both cells such that A’s efficiency, as one of the cells firing B, is increased” (Hebb 1949). Although Hebb stated that this idea is old, strengthening synapses (that is, increasing synaptic efficacy or weight) connecting co-active neurons has since been called “Hebbian plasticity”. It is also called Long-Term Potentiation (LTP).

Even though Hebb wrote that “less strongly established memories would gradually disappear unless reinforced through a slow “synaptic decay” (Hebb 1949), he did not provide an active mechanism for weakening synapses. Hence, the synaptic strengths or “weights” are unbounded and it is not possible to forget previously learned patterns to learn new ones. The first solution proposed a few years later was to maintain the sum of synaptic weights in a neuron constant (Rochester et al. 1956). In 1982, Oja proposed a Hebbian-like rule (Oja 1982) that adds a “forgetting” parameter and solves the stability problem with a form of local multiplicative normalization for synaptic weights. In the same year, Bienenstock et al. (1982) proposed the Bienenstock Cooper Munro (BCM) learning rule where during pre-synaptic stimulation, low-frequency activity of the post-synaptic neuron leads to Long-Term Depression (LTD) while high-frequency activity would lead to LTP. This model was an important shift as it introduced the so-called homo-synaptic LTD, where the plasticity was determined by the post-synaptic spike rate with no requirement on the temporal order of spikes. The importance of the post-synaptic neuron in synaptic plasticity was further demonstrated by showing how post-synaptic sub-threshold depolarization can determine whether LTP or LTD is applied (Artola et al. 1990, Sjöström et al. 2001).

Time is inherently present in any associative learning since it only relies on co-occurring events. McNaughton et al. (1978) were the first to experimentally explore the importance of the pre- and post-synaptic spike timing in plasticity. Fifteen years later, Gerstner et al. (1993) hypothesized that these pre/post spike times contain more information for plasticity compared to spike rates. Their hypothesis would be confirmed by experiments conducted by Stuart & Sakmann (1994) who discovered that the post-synaptic spike is back-propagating into the dendrites, as well as by Markram et al. (1995) who showed that a single spike leaves behind a Calcium trace of about 100ms which is propagated back into the dendrites. These findings were highly influential in the field because they provided evidence that synapses have local access to the timings of pre-synaptic and postsynaptic neurons spikes. In their subsequent

experiments, Markram et al. (1995) provided additional evidence that precise timing is important in neocortical neurons: They showed that using a pre/post pairing with a time difference of 10 ms led to LTP, while using the same time difference of 10 ms in an inverted post/pre pairing led to LTD (Markram et al. 1997). Larger time differences of 100 ms did not lead to any change in the synaptic weights. Almost concurrently, Bi & Poo (1998) performed similar experiments and found a 40 ms coincidence time window using paired recordings. These experiments proved that in addition to mean rates, also spike-timing matters. This phenomenon was later formulated in a learning rule named Spike-Timing Dependent Plasticity (STDP) (Song et al. 2000).

In this respect, the Hebbian learning formula proposed by Shatz (1992) that “cells that fire together wire together” could be misleading, as Hebb’s (1949) postulate is directional: “axon of cell A is near enough to excite a cell B”, which may be interpreted as implicitly time-dependent since cell A has to fire before cell B. On the other hand, STDP had been later found to only partially explain more elaborate learning protocols, which showed that while both LTP and LTD are compatible STDP at low frequencies, only LTP occurs at high frequencies regardless of the temporal order of spikes (Sjöström et al. 2001). As pair-based STDP models do not reproduce the frequency dependence of synaptic plasticity, Pfister & Gerstner (2006) proposed Triplet-based STDP (T-STDP) rule where LTP and LTD depend on a combination of three pre- and post-synaptic spikes (either two pre- and one post or one pre- and two post). Both pair-based and triplet-based STDP were then shown to be able to reproduce BCM like behavior (Gjorgjieva et al. 2011). Furthermore, the same frequency dependent experiments (Sjöström et al. 2001) showed that the state of the post-synaptic membrane voltage is important for driving LTP or LTD under the same pre/post timing conditions, confirming previous studies on the role of the neuron membrane voltage in plasticity (Artola et al. 1990). Therefore, these recent findings supported the computational plasticity models that depend on the arrival of the pre-synaptic spike and the voltage of the postsynaptic membrane (Fusi, Annunziato, Badoni, Salamon & Amit 2000, Brader et al. 2007, Clopath et al. 2010), and which were also compatible with the STDP model. The more recent three-factor learning rules aim at bridging the gap between the different time scales of learning, specifically from pre-post spike timings (milliseconds) to behavioral time scales (seconds) (Gerstner et al. 2018).

Today, after more than two millennia of questioning, experimenting and more recently modeling, synaptic plasticity is still not fully understood and many questions remain unanswered. Nevertheless, it is clear that multiple forms of plasticity and time-scales co-exist in the synapse and in the whole brain (Nelson et al. 2002). They link to each other by sharing locality as a fundamental computational principle.

2.2. Experimental perspective

Synaptic weights are correlated with various elements in biological synapses (Bartol et al. 2015) such as the number of docked vesicles in the pre-synaptic terminal (Harris & Sultan 1995), the area of the pre-synaptic active zone (Schikorski & Stevens 1997), the dendritic spine head size (Harris & Stevens 1989, Hering & Sheng 2001), the amount of released transmitters (Murthy et al. 2001, Branco et al. 2008, Ho et al. 2011), the area of the post-synaptic density (Lisman & Harris 1994), and the number of AMPA receptors (Bourne et al. 2013, *Biology of Synaptic Plasticity* 2020). Synaptic plasticity is known to be heterogeneous across different types of synapses (Abbott &

Nelson 2000, Bi & Poo 2001), and there is no unified experimental protocol to confront the different observations. Here we present the experimental results that led to the bottom-up definition of multiple plasticity rules.

Spike-timing dependence. Multiple experiments have been performed to demonstrate the dependence of plasticity on the exact pre- and post-synaptic neurons spike times (Markram et al. 1997, Bi & Poo 1998, Sjöström et al. 2001). From a computational point of view, these experiments led to the proposal of the STDP learning rule (Abbott & Nelson 2000, Markram et al. 2011), and its variants, such as T-STDP (Pfister & Gerstner 2006). Typically in these experiments, a pre-synaptic neuron is driven to fire shortly before or shortly after a postsynaptic one, by injecting a current pulse to the specific soma at the desired time. Specifically, these pre-post and post-pre pairings are repeated for 50 to 100 times at a relatively low frequency of about 1 Hz to 10 Hz (Sjöström & Gerstner 2010). Experimental results reveal synaptic plasticity mechanisms that are sensitive to the difference in spike times at the time scale of milliseconds (Gerstner et al. 1993). LTP is observed when the pre-synaptic spike occurs within 10 ms before the post-synaptic spike is produced, while LTD is observed when the order is reversed (Markram et al. 1997, Bi & Poo 1998). In biology, this precise spike timing dependence could be supported by local processes in the synapses that have access to both the timing information of pre-synaptic spikes and to the postsynaptic spike times, either by sensing their local membrane voltage changes or by receiving large depolarizations caused by output spikes that are back-propagated into the dendrite (Stuart & Sakmann 1994).

Post-synaptic membrane voltage dependence. Another feature of synaptic plasticity is its dependence on the post-synaptic neuron membrane voltage (Artola et al. 1990). To study this dependence, the pre-synaptic neuron is driven to fire while the post-synaptic neuron is clamped to a fixed voltage. The clamped voltage level will determine the outcome of the synaptic changes: If the voltage is only slightly above the resting potential of the neuron, then LTD is observed while if it is higher, then LTP is observed (Artola et al. 1990, Ngezahayo et al. 2000). These experiments show that post-synaptic spikes are not strictly necessary to induce long-term plasticity (Lisman & Spruston 2005, Lisman & Spruston 2010). Moreover, even in the presence of a constant pre/post timing (10 ms) at low frequencies (0.1 Hz), the post-synaptic membrane voltage determines whether LTP or LTD can be induced (Sjöström et al. 2001, Sjöström & Gerstner 2010). These findings suggest that the post-synaptic membrane voltage might be more important than the pre/post spike timing for synaptic plasticity.

Frequency dependence. While both spike-timing and post-synaptic membrane voltage dependence are observed in experimental protocols when relatively low spike frequencies are used, at high frequencies LTP tends to dominate over LTD regardless of precise spike timing (Sjöström et al. 2001). This spike-rate dependence, which is correlated with the Calcium concentration of the postsynaptic neuron (Sjöström et al. 2001), is captured by multiple learning rules such as BCM (Bienenstock et al. 1982) or the T-STDP (Pfister & Gerstner 2006) rule. In these rules, high spike rates produce a strong / rapid increase in Calcium concentration that leads to LTP, while low spike rates produce a modest / slow increase in Calcium concentration

that decays over time and leads to LTD (Bliss & Collingridge 1993).

2.3. Theoretical perspective

Theoretical investigations of plasticity have yielded crucial insights in computational neuroscience. Here, we summarize the fundamental theoretical and practical requirements for long-term synaptic plasticity.

Sensitivity to pre-post spikes correlations. Synaptic plasticity has to adjust the synaptic weights depending on the correlation between the pre- and post-synaptic neurons (Hebb 1949). Depending on how information is encoded, this can be achieved using spike times, spike rates or both (Brette 2015). It is important to note that the objective behind the detection of correlation is to detect causality which would ensure a better prediction (Vigeneron & Martinet 2020). Even if correlation does not imply causality (Brette 2015), correlation can be considered as a tangible trace for causality in learning.

Selectivity to different patterns. In supervised, semi-supervised and reinforcement learning, post-synaptic neurons are driven by a specific teacher signal that forces target neurons to spike and other neurons to remain silent, allowing them to become selective to the pattern applied in input (Brader et al. 2007). In unsupervised learning, the selectivity emerges from competition among neurons (Kohonen 1990, Olshausen & Field 1996) like in Winner-Take-All (WTA) networks (Chen 2017). By associating local plasticity with a WTA network, it is possible to create internal models of the probability distributions of the input patterns. This can be interpreted as an approximate Expectation-Maximization algorithm for modeling the input data (Nessler et al. 2009). Recently, the combination of STDP with WTA networks has been successfully used for solving a variety of pattern recognition problems in both supervised (Chang et al. 2018) and unsupervised scenarios (Bichler et al. 2012, Diehl & Cook 2015, Iyer & Basu 2017, Rathi & Roy 2021).

Stability of synaptic memory. Long-term plasticity requires continuous adaptation to new patterns but it also requires the retention of previously learned patterns. As any physical system has a limited storage capacity, the presentation of new experiences will continuously generate new memories that would eventually lead to saturation of the capacity. When presenting new experiences, the stability (and retrieval) of old memories is a major problem in Artificial Neural Networks (ANNs). When learning of new patterns leads to the complete corruption or destruction of previously learned ones, then the network undergoes *catastrophic forgetting* (Nadal et al. 1986, French 1999). Both catastrophic forgetting and continual learning are critical problems that need to be addressed for always-on neural processing systems, including artificial embedded processors applied to solving edge-computing tasks. The main challenge in always-on learning is not its resilience against time, but its resilience against ongoing activity (Fusi et al. 2005).

Different strategies can be used to find a good balance between plasticity and stability. A first solution is to introduce stochasticity in the learning process, for example by using Poisson distributed spike trains to represent input signals to promote plasticity, while promoting stability using a bi-stable internal variable that slowly drives the weight between one of two possible stable states (Brader et al. 2007). As a

result, only a few synapses will undergo a LTP or LTD transition for a given input, to progressively learn new patterns without forgetting previously learned patterns. A second solution is to have an intrinsic stop-learning mechanism to modulate learning and not change synaptic weights if there is enough evidence that the current input pattern has already been learned.

Depending on the particular pattern recognition problem to be solved and the learning paradigm (offline/online), specific properties can be more or less important.

3. Computational primitives of synaptic plasticity

In this work, we refer to “computational primitives of synaptic plasticity” as those basic plasticity mechanisms that make use of local variables.

3.1. Local variables

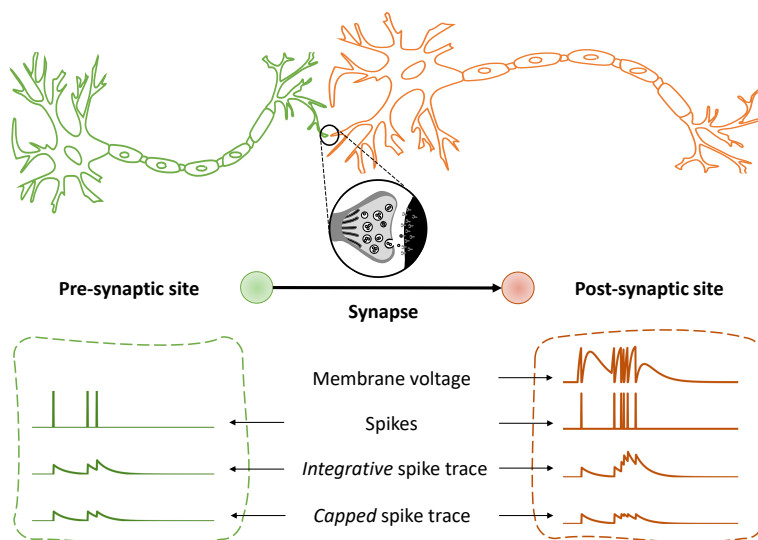


Figure 1: The local variables involved in the local synaptic plasticity models we review in this survey: Pre- and/or post-synaptic spike traces (capped or integrative) and post-synaptic membrane (dendritic or somatic) voltage.

The following are the local variables that we consider:

Pre- and post-synaptic spike traces: These are the traces generated at the pre- and post-synaptic site triggered by the spikes of the corresponding pre- or post-synaptic neurons. They can be computed by either integrating the spikes using a linear operator in models and a low-pass filter in circuits, or by using non-linear operators/circuits. Figure 1 shows examples both linear (denoted as “integrative”) and non-linear (denoted as “capped”) spike traces. In general, these traces represent the recent level of activation of the pre- and post-synaptic neurons. Depending on the learning rule, there might be one or more spike traces

per neuron with different decay rates. The biophysical substrates of these traces can be diverse (Pfister & Gerstner 2006, Graupner & Brunel 2010), for example reflecting the amount of bound glutamate (Karmarkar & Buonomano 2002) or the number of N-Methyl-D-Aspartate (NMDA) receptors in an activated state (Senn et al. 2001). The post-synaptic spike traces could reflect the Calcium concentration mediated through voltage-gated Calcium channels and NMDA channels (Karmarkar & Buonomano 2002), the number of secondary messengers in a deactivated state of the NMDA receptor (Senn et al. 2001) or the voltage trace of a back-propagating action potential (Shouval et al. 2002).

Post-synaptic membrane voltage: The post-synaptic neuron’s membrane potential is also a local variable, as it is accessible to all of the neuron’s synapses.

These local variables are the basic elements that can be used to induce a change in the synaptic weight, which is reflected in the change of the post-synaptic membrane voltage that a pre-synaptic spike induces.

3.2. Spikes interaction

We refer to spike interactions as the number of spikes from the past activity of the neurons that are taken into account for the weight update. In particular, we distinguish two spikes interaction schemes:

All-to-all: In this scheme, the spike trace is ”integrative” and influenced, asymptotically, by the whole previous spiking history of the pre-synaptic neuron. The contribution of each spike is expressed in the form of a Dirac delta which should be integrated. Nevertheless, if the spikes are considered to be point processes for which their spike width is zero in the limit, the contribution of all spikes in Eq. (1) can be approximated as follows:

$$\frac{dX(t)}{dt} = -\frac{X(t)}{\tau} + \sum_i A \delta(t - t_i) \quad (1)$$

where $\delta(t - t_i)$ is a spike occurring at time t_i , τ is the exponential decay time constant and A is the jump value such that at the moment of a spike event, *the spike trace jumps by A* . In addition to being a good first-order model of synaptic transmission, this transfer function can be easily implemented in electronic hardware using low-pass filters. Indeed, the trace $X(t)$ represents the online estimate of the neuron’s mean firing rate (Dayan & Abbott 2001).

Nearest spike: This is a non-linear mode in which the spike trace is only influenced by the most recent pre-synaptic spike. It is implemented by means of a hard bound that is limiting the maximum value of the trace, such that if the jumps reach it, the trace is ”capped” at that bound value. It is expressed in Eq. (2):

$$\frac{dX(t)}{dt} = -\frac{X(t)}{\tau} + \sum_i (A - X(t)) \delta(t - t_i) \quad (2)$$

where A is both the jump value and the hard bound, such that at the moment of a spike event, *the spike trace jumps to A* . It means that the spike trace gives an online estimate of the time since the last spike.

Therefore, the jump and bound parameters control the sensitivity of the learning rule to the spike timing and rate combined (all-to-all) or to the spike timing alone (nearest spike), while the decay time constant controls how fast the synapse forgets about these activities. Further spike interaction schemes are possible, for example by adapting the nearest spike interaction so that spike interactions producing LTP would dominate over those producing LTD.

3.3. Update trigger

In most synaptic plasticity rules, the weights update is event-based and happens at the moment of a pre-synaptic spike (e.g. Brader et al. 2007), post-synaptic spike (e.g. Diehl & Cook 2015) or both pre- and post-synaptic spikes (e.g. Song et al. 2000). This event-based paradigm is particularly interesting for hardware implementations, as it exploits the spatio-temporal sparsity of the spiking activity to reduce the energy consumption with less updates. On the other hand, some rules use a continuous update (e.g. Graupner & Brunel 2012) arguing for more biological plausibility, or a mixture of both with e.g. depression at the moment of a pre-synaptic spike and continuous potentiation (e.g. Clopath et al. 2010).

3.4. Synaptic weights

The synaptic weight represents the strength of a connection between two neurons. Synaptic weights have three main characteristics:

- (i) Type: Synaptic weights can be continuous, with full floating-point resolution in software, or with fixed/limited resolution (binary in the extreme case). Both cases can be combined by using fixed resolution synapses (e.g., binary synapses), which however have a continuous internal variable that determines if and when the synapse undergoes a low-to-high (LTP) or high-to-low (LTD) transition, depending on the learning rule.
- (ii) Bistability: In parallel to the plastic changes that update the weights, on their weight update trigger conditions, synaptic weights can be continuously driven to one of two stable states, depending on additional conditions on the weight itself and on its recent history. These bistability mechanisms have been shown to protect memories against unwanted modifications induced by ongoing spontaneous activity (Brader et al. 2007) and provide a way to implement stochastic selection mechanisms.
- (iii) Bounds: In any physical neural processing system, whether biological or artificial, synaptic weights have bounds: they cannot grow to infinity. Two types of bounds can be imposed on the weights: (1) hard bounds, in rules with additive updates independent of weight, or (2) soft bounds, in weight-dependent updates (for example, multiplicative) rules that drive the weights toward the bounds asymptotically (Morrison et al. 2008).

3.5. Stop-learning

An intrinsic mechanism to modulate learning and automatically switch from the training mode to the inference mode is important, especially in an online learning context. This “stop-learning” mechanism can be either implemented with a global signal related to the performance of the system, as in reinforcement learning, or

with a local signal produced in the synapses or in the soma. For example, a local variable that can be used to implement stop-learning could be derived from the post-synaptic neuron’s membrane voltage (Clopath et al. 2010, Albers et al. 2016) or spiking activity (Brader et al. 2007, Graupner & Brunel 2012).

4. Models of synaptic plasticity

We present a representative set of spike-based synaptic plasticity models, summarize their main features, and explain their working principles. Table 1 shows a direct comparison of the computational principles used by the relevant models, and Tables 14 and 15 show the main variables common to the different models.

Table 1: Spike-based local synaptic plasticity rules: comparative table

Plas- ticity rule	Local variables	Spikes inter- action	Update trigger (spike)		Synaptic weights			Stop- learning
			LTD	LTP	Type	Bista- bility	Bounds	
STDP	Pre- and post-synaptic spike traces	Nearest spike	Pre	Post	Analog	No	Hard	No
T-STDP	Pre-synaptic spike trace + 2 post-synaptic spike traces (different time constants)	Nearest spike / all-to-all	Pre	Post	Analog	No	Hard	No
SDSP	Post-synaptic membrane voltage + post-synaptic spike trace	All-to-all		Pre	Binary*	Yes	Hard	Yes ¹
V-STDP	Pre-synaptic spike trace + post-synaptic membrane voltage + 2 post-synaptic membrane voltage traces	All-to-all	Pre	Contin- uous	Analog	No	Hard	Yes ²
C-STDP	One synaptic spike trace updated by both pre- and post-synaptic spikes	All-to-all	Continuous		Analog	Yes	Soft	Yes ³
SBCM	Pre- and post-synaptic spike traces	All-to-all	Continuous		Analog	No	Hard	No
MPDP	Pre-synaptic spike trace + post-synaptic membrane voltage	All-to-all	Continuous		Analog	No	Hard	Yes ⁴
DPSS	Pre-synaptic spike trace + post-synaptic dendritic voltage + post-synaptic somatic spike	All-to-all	Continuous		Analog	No	Hard	No
RDSP	Pre-synaptic spike trace	All-to-all		Post	Analog	No	Soft	No
H-MPDP	Pre-synaptic spike trace + post-synaptic membrane voltage	All-to-all	Continuous		Analog	No	Hard	Yes ⁵
C-MPDP	Post-synaptic membrane voltage + post-synaptic spike trace	All-to-all		Pre	Analog	No	Hard	No
BDSP	Pre-synaptic spike trace + post-synaptic event trace + post-synaptic burst trace	All-to-all	Post (event)	Post (burst)	Analog	No	Hard	No

* Binary with analog internal variable.

¹ At low and high activities of post-neuron (post-synaptic spike trace).² At low low-pass filtered post-synaptic membrane voltage (post-synaptic membrane voltage trace).³ At low activity of pre- and post-neurons merged (synaptic spike trace).⁴ At medium (between two thresholds) internal update trace.⁵ At medium (between two thresholds) post-synaptic membrane voltage.

4.1. Song et al. (2000): Spike-Timing Dependent Plasticity (STDP)

Spike-Timing Dependent Plasticity (STDP) (Song et al. 2000) was proposed to model how pairs of pre-post spikes interact based solely on their timing. It is one of the most widely used synaptic plasticity algorithms in the literature.

$$\Delta w = \begin{cases} A_+ \exp(\frac{\Delta t}{\tau_+}) & \text{if } \Delta t < 0. \\ -A_- \exp(\frac{-\Delta t}{\tau_-}) & \text{if } \Delta t \geq 0. \end{cases} \quad (3)$$

The synaptic weight is updated according to Eq. (3), whose variables are described in Tab. 2. If a post-synaptic spike occurs after a pre-synaptic one ($\Delta t < 0$), potentiation is induced (triggered by the post-synaptic spike). In contrast, if a pre-synaptic spike occurs after a post-synaptic spike ($\Delta t \geq 0$), depression occurs (triggered by the pre-synaptic spike). The time constants τ_+ and τ_- determine the time window in which the spike interaction leads to changes in synaptic weight. As shown in Tab. 1, STDP is based on local pre- and post-spike traces with nearest spike interaction, meaning that the spike traces are capped. Fig. 2 illustrates how STDP is implemented using these spike traces for online learning.

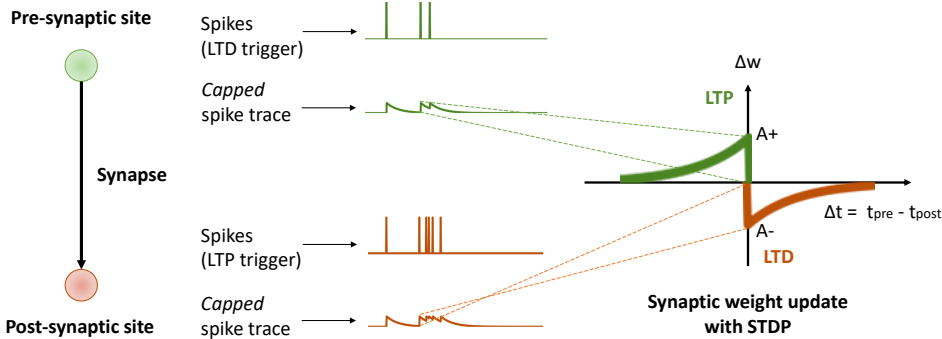


Figure 2: Online implementation principle of STDP using local pre- and post-synaptic capped spike traces which provide an online estimate of the time since the last spike. For example, at the moment of post-synaptic spike, potentiation is induced with a weight change that is proportional to the value of the pre-synaptic spike trace, and the post-synaptic spike trace is updated with a jump to A_- .

Table 2: Variables of the STDP rule.

Variable	Description
w	Synaptic weight
A_+ / A_-	Maximum amount of synaptic change
Δt	Time difference between pre- and post-synaptic spikes: $t_{pre} - t_{post}$
τ_+ / τ_-	Time constants of synaptic traces

4.2. Pfister and Gerstner (2006): Triplet-based STDP (T-STDP)

The main limitation of the original STDP model is that it is only time-based; thus, it cannot reproduce frequency effects as well as triplet and quadruplet experiments. In this work, Pfister & Gerstner (2006) introduces additional terms in the learning rule to expand the classical pair-based STDP to a Triplet-based STDP (T-STDP).

Specifically, the authors introduce a triplet depression (i.e. 2-pre and 1-post) and potentiation term (i.e. 1-pre and 2-post). They do this by adding four additional variables that they call detectors: r and o . r_1 and r_2 detectors are pre-synaptic spike traces which increase whenever there is a pre-synaptic spike and decrease back to zero with their individual intrinsic time constants. Similarly, o_1 and o_2 detectors increase on post-synaptic spikes and decrease back to zero with their individual intrinsic time constants. The weight changes are defined in Eqs. (4), whose variables are described in Tab. 3.

$$\begin{aligned} w(t) &\rightarrow w(t) + r_1(t) [A_2^+ + A_3^+ o_2(t - \epsilon)] & \text{if } t = t^{\text{post}} \\ w(t) &\rightarrow w(t) - o_1(t) [A_2^- + A_3^- r_2(t - \epsilon)] & \text{if } t = t^{\text{pre}} \end{aligned} \quad (4)$$

While in classical STDP, potentiation takes place shortly after a pre-synaptic spike and upon occurrence of a post-synaptic spike, in the current framework several conditions need to be considered. Potentiation is triggered at every post-synaptic spike where the weight change is gated by the r_1 detector and modulated by the o_2 detector. If there are no post-synaptic spikes shortly before the current one (o_2 is zero) the degree of potentiation is determined by A_2^+ only, just like in the pair-based STDP. If however a triplet of spikes occurs (in this case 1-pre and 2-post) o_2 is non zero and an additional potentiation term $A_3^+ o_2(t - \epsilon)$ contributes to the weight change. Analogously, r_2 , o_1 , A_2^- and A_3^- operate for the case of synaptic depression which is triggered at every pre-synaptic spike.

Table 3: Variables of the T-STDP rule.

Variable	Description
w	Synaptic weight
r_1 / r_2	Pre-synaptic spike traces - integrative
o_1 / o_2	Post-synaptic spike traces - integrative
A_2^+ / A_2^-	Weight change amplitude whenever there is a pair event
A_3^+ / A_3^-	Weight change amplitude whenever there is triplet event
ϵ	Small positive constant
$t^{\text{pre}} / t^{\text{post}}$	Time of pre- and post-synaptic spikes

4.3. Brader et al. (2007): Spike-Driven Synaptic Plasticity (SDSP)

The Spike-Driven Synaptic Plasticity (SDSP) learning rule addresses in particular the problem of memory maintenance and catastrophic forgetting: the presentation of new experiences continuously generates new memories that will eventually lead to saturation of the limited storage capacity, hence forgetting. As discussed in Sec. 2.3, this problem concerns all learning rules in an online context. SDSP attempts to solve it by slowing the learning process in an unbiased way. The model randomly selects the synaptic changes that will be consolidated among those triggered by the input, therefore learning to represent the statistics of the incoming stimuli.

The SDSP model proposed by Brader et al. (2007) is demonstrated in a feed-forward neural network used for supervised learning in the context of pattern classification. Nevertheless, the model is also well suited for unsupervised learning of patterns of activation in attractor neural networks (Del Giudice et al. 2003, Brader et al. 2007). It does not rely on the precise timing difference between pre- and post-synaptic spikes, instead the weight update is triggered by single pre-synaptic spikes. The sign of the weight update is determined by the post-synaptic neuron's membrane voltage $V(t^{pre})$. The post-synaptic neuron's Calcium variable $C(t^{pre})$ represents a trace of the recent low-pass filtered post-synaptic activity and is used to determine if synaptic updates should occur (stop-learning mechanism). The synaptic dynamics is described in Eq. (1).

The internal variable X is updated according to Eq. (5) with the variables described in Tab. 4.

$$\begin{aligned} X &\rightarrow X + a \text{ if } V(t^{pre}) > \theta_V \text{ and } \theta_{up}^l < C(t^{pre}) < \theta_{up}^h \\ X &\rightarrow X - b \text{ if } V(t^{pre}) \leq \theta_V \text{ and } \theta_{down}^l < C(t^{pre}) < \theta_{down}^h \end{aligned} \quad (5)$$

The weight update depends on the instantaneous values of $V(t^{pre})$ and $C(t^{pre})$ at the arrival of a pre-synaptic spike. A change of the synaptic weight is triggered by the pre-synaptic spike if $V(t^{pre})$ is above a threshold θ_v , provided that the post-synaptic Calcium trace $C(t^{pre})$ is between the potentiation thresholds θ_{up}^l and θ_{up}^h . An analogous but flipped mechanism induces a decrease in the weights.

The synaptic weight is restricted to the interval $0 \leq X \leq X_{max}$. The bistability on the synaptic weight implies that the internal variable X drifts (and is bounded) to either a low state or a high state, depending on whether X is below or above a threshold θ_X respectively. This is shown in Eqs (6).

$$\frac{dX}{dt} = \begin{cases} \alpha & \text{if } X > \theta_X \\ -\beta & \text{if } X \leq \theta_X \end{cases} \quad (6)$$

Table 4: Variables of the SDSP rule.

Variable	Description
X	Synaptic weight
a, b	Jump sizes
$V(t)$	Post synaptic membrane potential
θ_V	Membrane potential threshold
$C(t)$	Post-synaptic spike trace (Calcium) - integrative
$\theta_{\text{up}}^l / \theta_{\text{up}}^h / \theta_{\text{down}}^l / \theta_{\text{down}}^h$	Thresholds on the Calcium variable
X_{max}	Maximum synaptic weight
α / β	Bistability rates, $\in \mathbb{R}^+$
θ_X	Bistability threshold on the synaptic weight

4.4. Clopath et al. (2010): Voltage-based STDP (V-STDP)

The Voltage-based STDP (V-STDP) rule has been introduced to unify several experimental observations such as post-synaptic membrane voltage dependence, pre-post spike timing dependence and post-synaptic rate dependence (Clopath & Gerstner 2010), but also to explain the emergence of some connectivity patterns in the cerebral cortex (Clopath et al. 2010). In this model, depression and potentiation are two independent mechanisms whose sum produces the total synaptic change. Variables of the equations are described in Tab. 5.

Depression is triggered by the arrival of a pre-synaptic spike ($X(t) = 1$) and is induced if the voltage trace $\bar{u}_-(t)$ of the post-synaptic membrane voltage $u(t)$ is above the threshold θ_- (see Eq. (7)).

$$\frac{dw^-}{dt} = -A_{\text{LTD}} X(t) [\bar{u}_-(t) - \theta_-]_+ \quad (7)$$

On the other hand, potentiation is continuous and occurs following Eq. (8) if the following conditions are met at the same time:

- The instantaneous post-synaptic membrane voltage $u(t)$ is above the threshold θ_+ , with $\theta_+ > \theta_-$;
- The low-pass filtered post-synaptic membrane voltage \bar{u}_+ is above θ_- ;
- A pre-synaptic spike occurred a few milliseconds earlier and has left a trace \bar{x} .

$$\frac{dw^+}{dt} = +A_{\text{LTP}} \bar{x}(t) [u(t) - \theta_+]_+ [\bar{u}_+(t) - \theta_-]_+ \quad (8)$$

The total synaptic change is the sum of depression and potentiation expressed in Eqs. (7) and (8) respectively, within the weights' hard bounds 0 and w_{max} .

Table 5: Variables of the V-STDP rule.

Variable	Description
w	Synaptic weight
$X(t)$	Pre-synaptic spike train $X(t) = \sum_n \delta(t - t^n)$
$\delta(\cdot)$	Delta-Dirac function
t^n	Time of the n-th pre-synaptic spike
$u(t)$	Post-synaptic membrane voltage
$\bar{u}_-(t) / \bar{u}_+(t)$	Post-synaptic membrane voltage traces
$A_{\text{LTD}} / A_{\text{LTP}}$	Amplitudes for depression and potentiation
θ_- / θ_+	Thresholds
$[\cdot]_+$	Rectifying bracket $[x]_+ = x$ if $x > 0$, $[x]_+ = 0$ otherwise
$\bar{x}(t)$	Pre-synaptic spike trace - integrative
w_{max}	Weight max hard bound

4.5. Graupner and Brunel (2012): Calcium-based STDP (C-STDP)

Founded on molecular studies, Graupner & Brunel (2012) proposed a plasticity model (C-STDP) based on a transient Calcium signal. They model a single Calcium trace variable $c(t)$ which represents the linear sum of individual Calcium transients elicited by pre- and post-synaptic spikes at times t_i and t_j , respectively. The amplitudes of the transients elicited by pre- and post-synaptic spikes are given by C_{pre} and C_{post} , respectively, and $c(t)$ decays constantly towards 0.

In the proposed model, the synaptic strength is described by the synaptic efficacy $\rho \in [0 : 1]$, which is constantly updated according to Eq. (9), whose variables are described in Tab. 6. Changes in synaptic efficacy are continuous and depend on the relative times in which the Calcium trace $c(t)$ is above the potentiation (θ_p) and depression (θ_d) thresholds (Graupner & Brunel 2012).

$$\tau \frac{d\rho}{dt} = -\rho(1 - \rho)(\rho_\star - \rho) + \gamma_p(1 - \rho)\Theta[c(t) - \theta_p] - \gamma_d\rho\Theta[c(t) - \theta_d] + \text{Noise}(t) \quad (9)$$

If the Calcium variable is above the threshold for potentiation ($\Theta[c(t) - \theta_p] = 1$) the synaptic efficacy is continuously increased by $\frac{\gamma_p(1-\rho)}{\tau}$ and as long as the Calcium variable is above the threshold for depression ($\Theta[c(t) - \theta_d] = 1$) the synaptic efficacy is continuously decreased by $-\frac{\gamma_d\rho}{\tau}$. Eventually, the efficacy updates induced by the Calcium concentration are in direct competition with each other as long as $c(t)$ is above both thresholds (Graupner & Brunel 2012). In addition to constant potentiation or depression updates, the bistability mechanism $-\rho(1 - \rho)(\rho_\star - \rho)$ drives the synaptic strength toward 0 or 1, depending on whether the instantaneous value of ρ is below or above the bistability threshold ρ_\star .

Graupner & Brunel (2012) show that their rule replicates a plethora of dynamics found in numerous experiments, including pair-based behavior STDP with different STDP curves, synaptic dynamics found in CA3-CA1 slices for postsynaptic neuron spikes and dynamics based on spike triplets or quadruplets. However, the rule contains only a single Calcium trace variable $c(t)$ per synapse, which is updated by both pre- and post-synaptic spikes. Since the synaptic efficacy update only depends on this

variable and not on the individual or paired spike events of the pre- and post-synaptic neuron, the system can get into a state in which isolated pre-synaptic or isolated post-synaptic activity can lead to synaptic efficacy changes. In extreme cases, isolated pre(post)-synaptic spikes could drive a highly depressed ($\rho = 0$) synapse into the potentiated state ($\rho = 1$), without the occurrence of any post(pre)-synaptic action potential. In a recent work, Chindemi et al. (2022) uses a modified version of the C-STDP rule based on data-constrained post-synaptic Calcium dynamics according to experimental data. They show that the rule is able to replicate the connectivity of pyramidal cells in the neocortex, by adapting the probabilistic and limited release of Ca^{2+} during pre- and post-synaptic activity.

Table 6: Variables of the C-STDP rule.

Variable	Description
$c(t)$	Pre- and post-synaptic spike trace (Calcium) - integrative
$C_{\text{pre}} / C_{\text{post}}$	Amplitudes of pre- and post-synaptic Calcium jumps
θ_p / θ_d	Thresholds for potentiation and depression
τ	Time constant of synaptic efficacy changes
ρ	Synaptic efficacy
ρ_\star	Bistability threshold on the synaptic efficacy
γ_p / γ_d	Rates of synaptic potentiation and depression
$\Theta[.]$	Heaviside function $\Theta[x] = 1$ if $x > 0$, $\Theta[x] = 0$ otherwise
Noise(t)	Activity-dependent noise

4.6. Bekolay et al. (2013): Spiking BCM (SBCM)

The Spiking BCM (SBCM) learning rule (Bekolay et al. 2013) has been proposed as another spike-based formulation of the abstract learning rule BCM, after the T-STDP rule. The weight update of the SBCM learning rule is continuous and is expressed in Eq. (10), whose variables are described in Tab. 7.

$$\Delta w_{ij} = \kappa \alpha_j a_i a_j (a_j - \theta(t)) \quad (10)$$

The mechanistic properties of SBCM are closer to the formal BCM rule, with the activities of the neurons expressed as spike activity traces and a filtered modification threshold. Nevertheless, the SBCM exhibits both the timing dependence of STDP and the frequency dependence of the T-STDP rule.

Table 7: Variables of the SBCM rule.

Variable	Description
w_{ij}	Synaptic weight between pre- and post-synaptic neurons i and j , respectively
κ	Learning rate
α_j	Scaling factor (gain) associated with the neuron
a_i / a_j	Pre- and post-synaptic spike traces
$\theta(t)$	Modification threshold: $\theta(t) = e^{-t/\tau} \theta(t-1) + (1 - e^{-t/\tau}) a_j(t)$
τ	Time constant of modification threshold

4.7. Yger and Harris (2013): Membrane Potential Dependent Plasticity (MPDP)

The Membrane Potential Dependent Plasticity (MPDP) rule, also called the “Convallis” rule (Yger & Harris 2013) aims to approximate a fundamental computational principle of the neocortex and is derived from principles of unsupervised learning algorithms. The main assumption of the rule is that projections with non-Gaussian distributions are more likely to extract useful information from real-world patterns (Hyvärinen & Oja 2000). Therefore, synaptic changes should tend to increase the skewness of a neuron’s sub-threshold membrane potential distribution. The rule is therefore derived from an objective function that measures how non-Gaussian the membrane potential distribution is, such that the post-synaptic neuron is often close to either its resting potential or spiking threshold (and not in between).

The resulting plasticity rule reinforces synapses that are active during post-synaptic depolarization and weakens those active during hyper-polarization. It is expressed in Eq. (11), where changes are continuously made on an internal update trace Ψ , and are then applied on the synaptic weight w as expressed in Eq. (12). The variables of the equations are explained in Tab. 8. The rule was used for unsupervised learning of speech data, where an additional mechanism was implemented to maintain a constant average firing rate.

$$\Psi(t) = \int_{-\infty}^t e^{-(t-\tau)/T} F'(V(\tau)) \sum_{i=1}^{N_s} K(\tau - t_i^s) d\tau \quad (11)$$

$$\frac{dw}{dt} = \begin{cases} \Psi - \theta_{\text{pot}} & \text{if } \theta_{\text{pot}} < \Psi \\ 0 & \text{if } \theta_{\text{dep}} < \Psi \leq \theta_{\text{pot}} \\ \Psi - \theta_{\text{dep}} & \text{if } \Psi \leq \theta_{\text{dep}} \end{cases} \quad (12)$$

Table 8: Variables of the MPDP rule.

Variable	Description
Ψ	Internal spike trace
T	Decay time constant
$F'(V(\tau))$	Function of the post-synaptic membrane voltage
$V(\tau)$	Post-synaptic membrane voltage
N_s	Pre-synaptic spike indices
$\sum_{i=1}^{N_s} K(\tau - t_i^s)$	Pre-synaptic spike trace - integrative
$K(\tau - t_i^s)$	Kernel for pre-synaptic spikes
w	Synaptic weight
$\theta_{\text{pot}} / \theta_{\text{dep}}$	Thresholds for potentiation and depression

4.8. Urbanczik and Senn (2014): Dendritic Prediction of Somatic Spiking (DPSS)

Urbanczik & Senn (2014) proposed a new learning model based on the Dendritic Prediction of Somatic Spiking (DPSS), which aims to implement a biologically plausible non-Hebbian learning rule. In their rule, they rely on the pre-synaptic spike trace, the post-synaptic spike event and the post-synaptic dendritic voltage of a multi-compartment neuron model. Plasticity in dendritic synapses is realizing a predictive coding scheme that matches the dendritic potential to the somatic potential.

This minimizes the error of dendritic prediction of somatic spiking activity of a conductance-based neuron model, that exhibits probabilistic spiking (Urbanczik & Senn 2014). The neuron membrane potential U is influenced by both a scaled version of the dendritic compartment potential V_w^* and the teaching inputs from excitatory or inhibitory proximal synapses I_U^{som} .

In their proposed learning rule (see Eq. (13)), the aim is to minimize the error between the predicted somatic spiking activity based on the dendritic potential $\phi(V_w^*(t))$ and the real somatic spiking activity represented by back-propagated spikes $S(t)$. The equation's variables are described in Tab. 9. The error $S(t) - \phi(V_w^*(t))$ is assigned to individual dendritic synapses based on their recent activation, similar to Yger & Harris (2013) and Albers et al. (2016).

$$PI_i(t) = [S(t) - \phi(V_w^*(t))]h(V_w^*(t))PSP_i(t) \quad (13)$$

Since the back-propagated spikes $S(t)$ are only 0 or 1, but the predicted rate $\phi(V_w^*)$ based on a sigmoidal function is never 0 or 1, PI will never be 0. In this case, there is never a zero weight change (Urbanczik & Senn 2014). The plasticity induction variable PI_i is continuously updated and used as an intermediate variable, before it is applied to induce a scaled persistent synaptic change, as expressed in Eq. (14).

$$\begin{aligned} \tau_\Delta \frac{d\Delta_i}{dt} &= PI_i(t) - \Delta_i \\ \frac{dw_i}{dt} &= \eta \Delta_i \end{aligned} \quad (14)$$

Sacramento et al. (2018) showed later analytically that the Dendritic Prediction of Somatic Spiking (DPSS) learning rule combined with similar dendritic predictive plasticity mechanisms approximate the error back-propagation algorithm, and demonstrated the capabilities of such a learning framework to solve regression and classification tasks.

Table 9: Variables of the DPSS rule.

Variable	Description
U	Somatic potential
V_w^*	Scaled dendritic potential
I_U^{som}	Proximal input current
$\phi(\cdot)$	Sigmoid function
$S(t)$	Back-propagated somatic spiking activity
$PI_i(t)$	Plasticity induction variable
$h(\cdot)$	Positive weighting function
$PSP_i(t)$	Pre-synaptic spike trace - integrative $PSP_i(t) = \sum_{s \in X_i^{\text{dnd}}} \kappa(t - s)$
$\kappa(t - s)$	Kernel for pre-synaptic spikes
X_i^{dnd}	Pre-synaptic spike train
w_i	Synaptic strength of synapse i
τ_Δ	Plasticity induction variable time constant
η	Learning rate

4.9. Diehl and Cook (2015): Rate Dependent Synaptic Plasticity (RDSP)

Diehl & Cook (2015) proposed the Rate Dependent Synaptic Plasticity (RDSP) rule as a local credit assignment mechanism for unsupervised learning in self-organizing Spiking Neural Networks (SNNs). The idea is to potentiate or depress the synapses for which the pre-synaptic neuron activity was high or low at the moment of a post-synaptic spike, respectively. The RDSP learning rule relies solely on the pre-synaptic information and is triggered when a post-synaptic spike arrives. The weight update is shown in Eq. (15), whose variables are described in Tab. 10.

$$\Delta w = \eta(x_{\text{pre}} - x_{\text{tar}})(w_{\text{max}} - w)^u \quad (15)$$

u determines the weight dependence of the update for implementing a soft bound, while the target value of the pre-synaptic spike trace x_{tar} is crucial in this learning rule because it acts as a threshold between depression and potentiation. If it is set to 0, then only potentiation is observed. It is hence important to set it to a non-zero value to ensure that pre-synaptic neurons that rarely lead to the firing of the post-synaptic neuron will become more and more disconnected. More generally, the higher the value of x_{tar} value, the more depression occurs and the lower the synaptic weights will be (Diehl & Cook 2015).

This rule was first proposed as a more biologically plausible version of a previously proposed rule for memristive implementations by Querlioz et al. (2013). The main difference between the two models is that the RDSP rule uses an exponential time dependence for the weight change which is more biologically plausible (Abbott & Song 1999) than a time-independent weight change. This can also be more useful for pattern recognition depending on the temporal dynamics of the learning task.

Table 10: Variables of the RDSP rule.

Variable	Description
w	Synaptic weight
η	Learning rate
x_{pre}	Pre-synaptic spike trace - integrative
x_{tar}	Target value of the pre-synaptic spike trace
w_{max}	Maximum weight
u	Weight dependence - soft bound

4.10. Albers et al. (2016): Homeostatic MPDP (H-MPDP)

The Homeostatic MPDP (H-MPDP) learning rule proposed by Albers et al. (2016) is derived from an objective function similar to that of the MPDP rule but with opposite sign, as it aims to balance the membrane potential of the post-synaptic neuron between two fixed thresholds; the resting potential and the spiking threshold of the neuron. Hence, the MPDP and the H-MPDP implement a Hebbian or homeostatic mechanism, respectively. In addition, the H-MPDP differs from the other described models by inducing plasticity only to inhibitory synapses.

Albers et al. (2016) use a conductance based neuron and synapse model, similar to the C-MPDP and the DPSS rules. The continuous weight updates of the H-MPDP

rule depend on the instantaneous membrane potential $V(t)$ and the pre-synaptic spike trace $\sum_k \epsilon(t - t_i^k)$ as expressed in Eq. (16) whose variables are described in Tab. 11.

$$w_i = \eta(-\gamma[V(t) - \vartheta_D]_+ + [\vartheta_P - V(t)]_+) \sum_k \epsilon(t - t_i^k) \quad (16)$$

The authors claim that their model is able to learn precise spike times by keeping a homeostatic membrane potential between two thresholds. This definition differs from the homeostatic spike rate definition of the C-MPDP rule by Sheik et al. (2016).

Table 11: Variables of the H-MPDP rule.

Variable	Description
w_i	Synaptic weight
η	Learning rate
γ	Scaling factor for LTD/LTP
$[\cdot]_+$	Rectifying bracket $[x]_+ = x$ if $x > 0$, $[x]_+ = 0$ otherwise
$V(t)$	Instantaneous membrane potential
ϑ_P/ϑ_D	Thresholds for plasticity induction
$\sum_k \epsilon(t - t_i^k)$	Pre-synaptic spike trace - integrative
t_i^k	Time of the k-th spike at the i-th synapse
$\epsilon(s)$	Kernel for pre-synaptic spikes

4.11. Sheik et al. (2016): Calcium-based MPDP (C-MPDP)

The Calcium-based MPDP (C-MPDP) learning rule (Sheik et al. 2016) was proposed with the explicit intention to have a local spike-timing based rule that would be sensitive to the order of spikes arriving at different synapses and that could be ported onto neuromorphic hardware.

Similarly to the DPSS rule, the C-MPDP rule uses a conductance-based neuron model. However, instead of relying on mean rates, it relies on the exact timing of the spikes. Furthermore, as for the H-MPDP rule, Sheik et al. (2016) propose to add a homeostatic element to the rule that targets a desired output firing rate. This learning rule is very hardware efficient because it depends only on the pre-synaptic spike time and not on the post-synaptic one. The equation that governs its behavior is Eq. (17). The weight update, triggered by the pre-synaptic spike, depends on a membrane voltage component (see Eq. (18)) and on a homeostatic one (see Eq. (19)). All equation variables are described in Tab. 12.

$$\Delta W = \Delta W_v + \Delta W_h \quad (17)$$

$$\Delta W_v = [\delta(V_m(t+1) > V_{\text{th}})\eta_+ - \delta(V_m(t+1) < V_{\text{th}})\eta_-]S(t - t_{\text{pre}}) \quad (18)$$

$$\Delta W_h = \eta_h(Ca_t - Ca)S(t - t_{\text{pre}}) \quad (19)$$

The post-synaptic membrane voltage dependent weight update shown in Eq. (18) depends on the values of the membrane voltage V_m and an externally set threshold V_{th} , which determines the switch between LTP and LTD. The homeostatic weight update

in Eq. (19) is proportional to the difference in post-synaptic activity represented by the post-synaptic spike trace Ca and an externally set threshold Ca_t .

The authors show that this learning rule, using the spike timing together with conductance based neurons, is able to learn spatio-temporal patterns in noisy data and differentiate between inputs that have the same 1st-moment statistics but different higher moment ones. Although they gear the rule toward neuromorphic hardware implementations, they do not propose circuits for the learning rule.

Table 12: Variables of the C-MPDP rule.

Variable	Description
W	Synaptic weight
ΔW_v	Voltage-based weight update
ΔW_h	Homeostatic weight update
δ	Boolean variable
V_m	Membrane potential
V_{th}	Threshold on membrane potential
$\eta_+ / \eta_- / \eta_h$	Magnitude of LTP/LTD/Homeostasis
$S(t - t_{\text{pre}})$	Pre-synaptic spike trains
t_{pre}	Pre-synaptic spike time
Ca	Post-synaptic spike trace (Calcium) - integrative
Ca_t	Calcium target concentration trace

4.12. Payeur et al. (2021): Burst-Dependent Synaptic Plasticity (BDSP)

The Burst-Dependent Synaptic Plasticity (BDSP) learning rule (Payeur et al. 2021) has been proposed to enable online, local, spike-based solutions to the credit assignment problem in hierarchical networks (Zenke & Neftci 2021), i.e. how can neurons high up in a hierarchy signal to other neurons, sometimes multiple synapses apart, whether to engage in LTP or LTD to improve behavior. The BDSP learning rule is formulated in Eq. (20) whose variables are described in Tab. 13.

$$\frac{dw_{ij}}{dt} = \eta[B_i(t) - \bar{P}_i(t)E_i(t)]\tilde{E}_j(t) \quad (20)$$

where an event $E_i(t)$ is said to occur either at the time of an isolated spike or at the time of the first spike in a burst, whereas a burst $B_i(t)$ is defined as any occurrence of at least two spikes (at the second spike) with an inter-spike interval less than a pre-defined threshold. Any additional spike within the time threshold belongs to the same burst. Hence, LTP and LTD are triggered by a burst and an event, respectively. Since a burst is always preceded by an event, every potentiation is preceded by a depression. However, the potentiation through the burst is larger than the previous depression, which results in an overall potentiation.

The moving average $\bar{P}_i(t)$ regulates the relative strength of burst-triggered potentiation and event-triggered depression. It has been established that such a mechanism exists in biological neurons (Mäki-Marttunen et al. 2020). It is formulated as a ratio between averaged post-synaptic burst and event traces. The authors show that manipulating the moving average $\bar{P}_i(t)$ (i.e. the probability that an event becomes

a burst) controls the occurrence of LTP and LTD, while changing the pre- and post-synaptic event rates simply modifies the rate of change of the weight while keeping the same transition point between LTP and LTD. Hence, the BDSP rule paired with the control of bursting provided by apical dendrites enables a form of top-down steering of synaptic plasticity in an online, local and spike-based manner.

Moreover, the authors show that this dendrite-dependent bursting combined with short-term plasticity supports multiplexing of feed-forward and feedback signals, which means that the feedback signals can steer plasticity without affecting the communication of bottom-up signals. Taken together, these observations show that combining the BDSP rule with short-term plasticity and apical dendrites can provide a local approximation of the credit assignment problem. In fact, the learning rule has been shown to implement an approximation of gradient descent for hierarchical circuits and achieve good performance on standard machine learning benchmarks.

Table 13: Variables of the BDSP rule.

Variable	Description
w_{ij}	Synaptic weight between pre- and post-synaptic neurons j and i
η	Learning rate
$B_i(t)$	Post-synaptic bursts
$\bar{P}_i(t)$	Exponential moving average of the proportion of post-synaptic bursts
$E_i(t)$	Post-synaptic events
$\tilde{E}_j(t)$	Pre-synaptic spike trace

4.13. Models common variables

Tables 14 and 15 show the major common variables between the different models. This allows an easy comparison of the formalism of each rule.

Table 14: Variables in common between rules Part I

Variables	STDP	T-STDP	SDSP	V-STDP	C-STDP	SBCM
Synaptic weight	w	w	X	w	ρ	w_{ij}
Weight bounds			X_{max}	w_{max}	$0 / 1$	
Traces		$o_1 / o_2 / r_1 / r_2$	$C(t)$	$\bar{u}_-(t) / \bar{u}_+(t) / \bar{x}(t)$	$c(t)$	a_i / a_j
Time constants	τ_+ / τ_-				τ	τ
Membrane potential			$V(t)$	$u(t)$		
Thresholds			$\theta_V / \theta_{up}^l / \theta_{up}^h / \theta_{down}^h / \theta_X$	θ_- / θ_+	$\rho_\star / \theta_p / \theta_d$	θ
Amplitudes	A_+ / A_-	$A_{2+} / A_{2-} / A_{3+} / A_{3-}$	$a / b / \alpha / \beta$	A_{LTP} / A_{LTD}	$C_{pre} / C_{post} / \gamma_p / \gamma_d$	κ / α_j

Table 15: Variables in common between rules Part II

Variables	MPDP	DPSS	RDSP	H-MPDP	C-MPDP	BDSP
Synaptic weight	w	w_i	w	w_i	W	w_{ij}
Weight bounds			w_{max}			
Traces	$\Psi / K(\tau - t_i^s)$	$PSP_i(t) / \Delta_i$	x_{pre}	$\sum_k \epsilon(t - t_i^k)$	Ca / Ca_t	$\widetilde{E}_j(t)$
Time constants	T	τ_Δ				
Membrane potential	$V(\tau)$	U		$V(t)$	V_m	
Thresholds	$\theta_{dep} / \theta_{pot}$		x_{tar}	$\vartheta_P / \vartheta_D$	V_{lth}	
Amplitudes		η	η / u	η / γ	$\eta_+ / \eta_- / \eta_h$	$\eta / \overline{P_i}(t)$

5. CMOS implementations of synaptic plasticity

Our comparison of plasticity models has highlighted many common functional primitives that are shared among the rules. These primitives can be grouped according to their function into the following blocks: low-pass filters, eligibility traces, and weight updates. These blocks can be readily implemented in CMOS technology, and they can be combined to implement different learning circuits. An overview of the proposed CMOS learning circuits that implement some of the models discussed is shown in Table 16. To better link the CMOS implementations with the models presented, we named all the current and voltage variables of our circuits to match those in the model equations.

5.1. CMOS building blocks

The basic building blocks found required for building neuromorphic learning circuits can be grouped in four different families.

Eligibility trace blocks These are implemented using either a current-mode integrator circuit, such as the Differential Pair Integrator (DPI), or other non-linear circuits that produce slowly decaying signals. Input spikes can either increase the trace amplitude, decrease it, or completely reset it. The rate at which the trace decays back to its resting state can be typically modulated with externally controllable parameters. Circuit blocks implementing eligibility traces are highlighted in green in the schematics.

Comparator blocks They are typically implemented using Winner-Take-All (WTA) current mode circuits, or voltage mode transconductance or Operational Amplifiers (OpAmps). The comparator block changes its output based on which

input is greater. Circuit blocks implementing comparators are highlighted in yellow in the schematics.

Weight update blocks They typically comprise a capacitor that stores a voltage related to the amplitude of the weight. Charging and discharging pathways connected to the capacitor enable potentiation and depression of the weight depending on the status of other signals. These blocks are is similar to the eligibility trace ones, except for the fact that they can produce both positive and negative changes. Circuit blocks implementing weight updates are highlighted in purple in the schematics.

Bistability blocks These are typically implemented using a Transconductance Amplifier (TA) connected in feedback operation which compares the weight voltage to a reference voltage. Depending on the value of the weight voltage the bistability circuit will push the weight to the closest stable state. In its simplest form they have one single reference voltage, but they could be expanded to produce multiple stable states. Circuit blocks implementing bistability are highlighted in red in the schematics.

Table 16: Neuromorphic circuits for spike-based local synaptic plasticity models

Rule	Paper	Difference with the model	Implementation
STDP	(Bofill-i-Petit et al. 2001) ¹	/	0.6 μm Fabricated
	(Indiveri 2002)	All-to-all spike interaction + bistable weights	1.5 μm Fabricated
	(Bofill-i-Petit & Murray 2004)	/	0.6 μm Fabricated
	(Cameron et al. 2005)	Anti-STDP + Non-exponential spike trace	0.35 μm Fabricated
	(Indiveri et al. 2006)	Bistable weights	1.6 μm Fabricated
	(Arthur & Boahen 2006) ²	All-to-all interaction + binary weights	0.25 μm Fabricated
	(Koickal et al. 2007)	Soft bounds	0.6 μm Fabricated
	(Liu & Mockel 2008)	All-to-all spike interaction + asymmetric bounds (soft lower bound + hard upper bound)	0.35 μm Fabricated
	(Tanaka et al. 2009)	/	0.25 μm Fabricated
	(Bamford et al. 2012)	All-to-all spike interaction	0.35 μm Fabricated
	(Gopalakrishnan & Basu 2014)	All-to-all spike interaction + asymmetric bounds (soft lower bound + hard upper bound)	0.35 μm Fabricated
	(Mastella et al. 2020)	/	0.15 μm Simulated
	(Mayr et al. 2010)	/	Simulated
T-STDP	(Azghadi et al. 2013)	/	0.35 μm Simulated
	(Gopalakrishnan & Basu 2017)	/	0.35 μm Fabricated
SDSP	(Fusi, Annunziato, Badoni, Salamon & Amit 2000)	No post-synaptic spike trace + no stop-learning mechanism	1.2 μm Fabricated
	(Chicca & Fusi 2001)	No post-synaptic spike trace + no stop-learning mechanism	0.6 μm Fabricated
	(Chicca et al. 2003)	No post-synaptic spike trace + no stop-learning mechanism	0.6 μm Fabricated
	(Giulioni et al. 2008)	Analog weights	0.35 μm Fabricated
	(Mitra et al. 2009)	Analog weights	0.35 μm Fabricated
	(Chicca et al. 2014)	Analog weights	0.35 μm Fabricated
C-STDP	(Maldonado Huayaney et al. 2016)	Hard bounds	0.18 μm Fabricated
RDSP	(Häfliger et al. 1997)	Nearest spike interaction + reset of pre-synaptic spike trace at post-spike + very small soft bounds	2 μm Fabricated
	(Ramakrishnan et al. 2011)	Nearest spike interaction + asymmetric bounds (soft lower bound + hard upper bound)	0.35 μm Fabricated

¹ Potentiation and depression triggers done with digital logic gates.² Weight storage in digital SRAM.

5.2. Spike-Timing Dependent Plasticity (STDP)

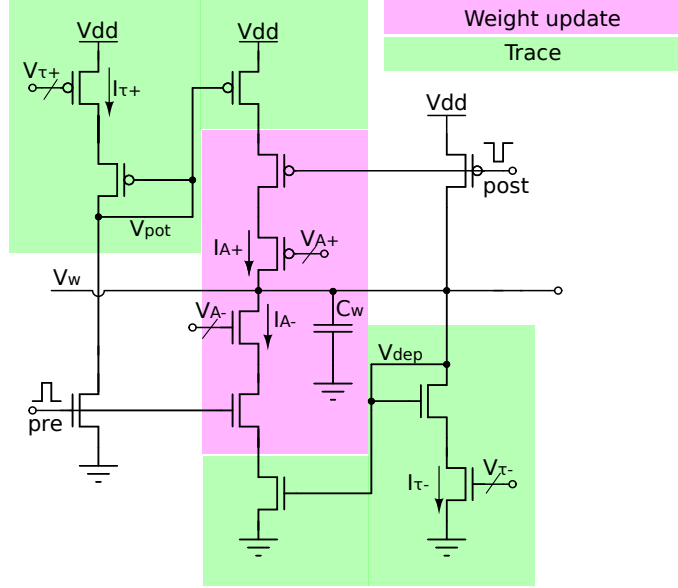


Figure 3: STDP circuit with highlighted the CMOS building blocks used: Eligibility traces (in green) and Weight updates (in violet). The voltage and current variables reflect the model equation. Adapted from: Indiveri et al. (2006).

Following the formalization of the STDP model in 2000 (see Eq. (3)), many CMOS implementations have been proposed. Most implement the model as explained in Section above (Bofill-i-Petit et al. 2001, Indiveri 2003, Bofill-i-Petit & Murray 2004, Arthur & Boahen 2006, Bamford et al. 2012) however, some exploit the physics of single transistors to propose a floating gate implementation (Liu & Mockel 2008, Gopalakrishnan & Basu 2014).

Indiveri et al. (2006) presented the implementation in Fig. 3. This circuit increases or decreases the analog voltage V_w across the capacitor C_w depending on the relative timing of the pulses *pre* and *post*. Upon arrival of a pre-synaptic pulse *pre*, a potentiating waveform V_{pot} is generated within the pMOS-based trace block (see Fig. 3). V_{pot} has a sharp onset and decays linearly with an adjustable slope set by $V_{\tau+}$. V_{pot} serves to keep track of the most recent pre-synaptic spike. Analogously, when a post-synaptic spike (*post*) occurs, V_{dep} and $V_{\tau-}$ create a trace of post-synaptic activity. By ensuring that V_{pot} and V_{dep} remain below the threshold of the transistors they are connected to and the exponential current-voltage relation in the sub-threshold regime, the exponential relationship to the spike time difference Δt of the model is achieved. While V_{A+} and V_{A-} set the upper-bounds of the amount of current that can be injected or removed from C_w , the decaying traces V_{pot} and V_{dep} determine the value of I_{A+} or I_{A-} and ultimately the weight increase or decrease on the capacitor C_w within the weight update block (see Fig. 3).

5.3. Triplet-based STDP (T-STDP)

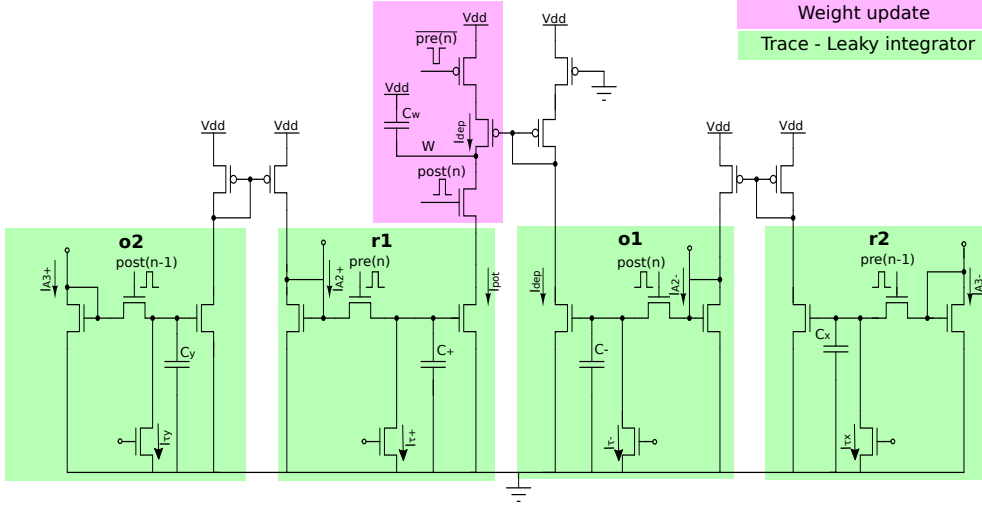


Figure 4: T-STDP circuit with highlighted the CMOS building blocks used: Eligibility traces with leaky integrators (in green) and weight updates (in violet). The voltage and current variables reflect the model equation. The r and o detectors of the model are also reported in this circuit figure. Adapted from: Azghadi et al. (2013).

Similarly, as for the pair-based STDP, there are many implementations of the T-STDP rule. While some are successful in implementing the equations in the model (Mayr et al. 2010, Meng et al. 2011, Rachmuth et al. 2011, Azghadi et al. 2013), others exploit the properties of floating gates (Gopalakrishnan & Basu 2017).

Specifically, Mayr et al. (2010) as well as Rachmuth et al. (2011) and Meng et al. (2011) implement learning rules that model the conventional pair-based STDP together with the BCM rule. Azghadi et al. (2013) is the first, to our knowledge, to not only model the function but also model the equations presented in Pfister et al. (2006) (see Eq. (4)). Figure 4 shows the circuit proposed by Azghadi in 2013 to model the T-STDP rule. It faithfully implements the equations by having independent circuits and biases, for the model parameters A_2^- , A_2^+ , A_3^- , and A_3^+ . These parameters correspond to spike-pairs or spike-triplets: post-pre, pre-post, pre-post-pre, and post-pre-post, respectively.

In this implementation, the voltage across the capacitor C_w determines the weight of the specific synapse. Here, a high potential at the node W is caused by a highly discharged capacitor indicating a low synaptic weight, which results in a depressed synapse. In the same way, a low potential at this node is caused by a more strongly charged capacitor and resembles a strong synaptic weight and in turn a potentiated synapse. The capacitor is charged and discharged by the two currents I_{pot} and I_{dep} respectively. These two currents are gated by the most recent pre- and post-synaptic spikes through the transistors controlled by $pre(n)$ and $post(n)$ within the weight update block (see Fig. 4)

The amplitude of the depression current I_{dep} and the potentiation current I_{pot} is given by the recent spiking activity of the pre- and post-synaptic neurons. On the arrival of a pre-synaptic spike, the capacitors C_+ and C_x (in the trace - leaky integrator blocks r1 and r2 in Fig. 4) are charged by the currents I_{A2+} and I_{A3-} . Analogously, the capacitors C_- and C_y (in the trace - leaky integrator blocks o1 and o2 in Fig. 4) are charged at the arrival of a post-synaptic spike by the currents I_{A2-} and I_{A3+} . Here, both currents I_{A2+} and I_{A2-} depend on an externally set constant input current plus the currents generated by the o2 and r2 blocks, respectively. These additional blocks o2 and r2 activated by previous spiking activity realize the triplet-sensitive behavior of the rule. All capacitors within the “Trace - leaky integrator” blocks (C_+ , C_- , C_x , C_y) constantly discharge with individual rates given by $I_{\tau+}$, $I_{\tau-}$, $I_{\tau x}$, $I_{\tau y}$, respectively.

5.4. Spike-Driven Synaptic Plasticity (SDSP)

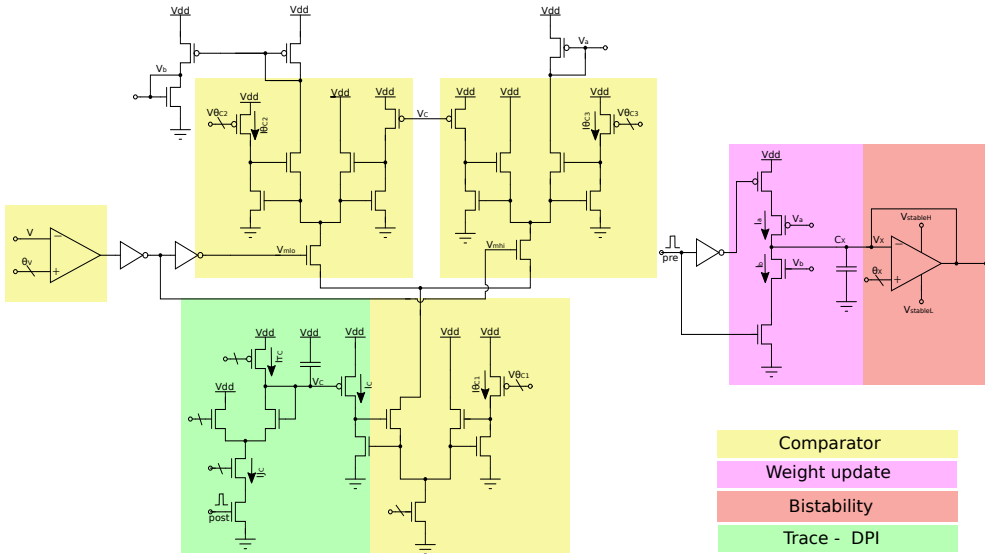


Figure 5: SDSP circuit with highlighted the CMOS building blocks used: Eligibility traces with a DPI (in green), weight updates (in violet), bistability (in red) and comparators with WTA (in yellow). The voltage and current variables reflect the model equation. Adapted from: Chicca et al. (2014).

A sequence of theoretical works on spike based learning rules designed in the theoretical framework of attractor neural network and mean field theory preceded the Spike-Driven Synaptic Plasticity (SDSP) formalization by Brader et al. (2007). Several hardware implementations by Fusi, Del Giudice & Amit (2000), Dante et al. (2001) and Chicca et al. (2003) accompanied this theoretical work. After formalization by Brader et al. (2007) many implementations of the Spike-Driven Synaptic Plasticity (SDSP) rule were proposed following the desire to build smarter, larger, and more autonomous networks. The implementations by Chicca et al. (2003), Mitra et al. (2009), Giulioni et al. (2008) and Chicca et al. (2014) share similar building blocks:

trace generators, comparators, blocks implementing the weight update and bistability mechanism. Here, we present the most complete design by Chicca et al. (2014), shown in Fig. 5, which replicates more closely the model equations (see Eq. (5)).

At each pre-synaptic spike *pre*, the weight update block (see Fig. 5) charges or discharges the capacitor C_x altering the voltage V_x , depending on the values of V_a and V_b . Here, V_x represents the synaptic weight. If $I_a > I_b$, V_x increases, while in the opposite case V_x decreases. Moreover, over long time scales, in the absence of pre-synaptic spikes, V_x is slowly driven toward the bistable states $V_{stableH}$ or $V_{stableL}$ depending on whether V_x is higher or lower than θ_x respectively (see bistability block in Fig. 5).

The V_a and V_b signals are continuously computed in the learning block, which compares the membrane potential of the neuron (V) to the threshold θ_V and evaluates in which region the Calcium concentration V_c lies. The neuron's membrane potential is compared to the threshold θ_V by a transconductance amplifier. If $V > \theta_V$, V_{mhi} is high and V_{mlo} is low, while if $V < \theta_V$, V_{mhi} is low and V_{mlo} is high. At the same time, the post-synaptic neuron spikes (*post*) are integrated by a DPI to produce the Calcium concentration V_c (see trace - DPI block in Fig. 5), which is then compared with three Calcium thresholds by three WTA circuits (see comparator circuits in Fig. 5). In the lower comparator, I_c is compared to $I_{\theta C1}$ and if $I_c < I_{\theta C1}$ no learning conditions of the SDSP rule is satisfied and there is no weight update. Assuming that $I_c > I_{\theta C1}$, the two upper comparators set the signals V_a and V_b . If V_{mlo} is high and $I_c < I_{\theta C2}$, V_b is increasing, setting the strength of the nMOS-based pull-down branch in the weight update block. If V_{mhi} is high and $I_c < I_{\theta C3}$, V_a is decreasing, setting the strength of the pMOS-based pull-up branch of the weight update block. These two branches in the weight update block are activated by the *pre* input spike.

5.5. Calcium-based STDP (C-STDP)

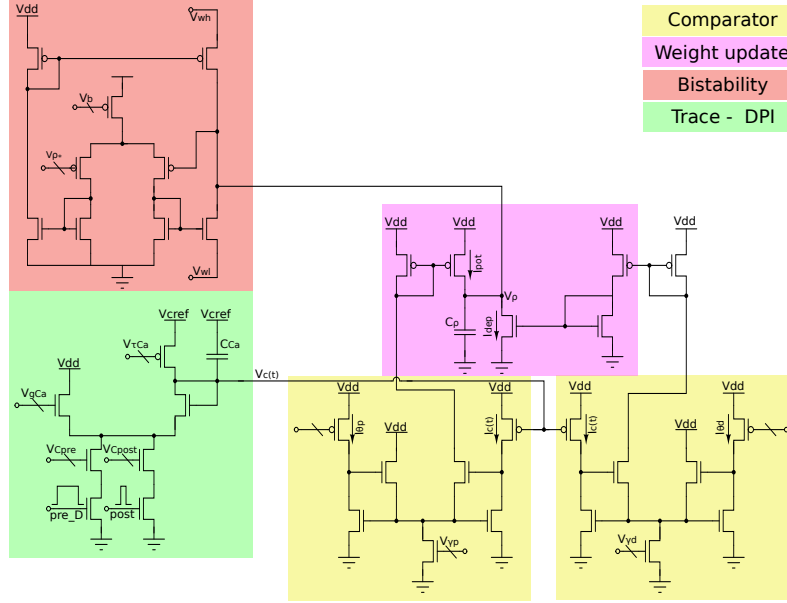


Figure 6: C-STDP circuit with highlighted CMOS building blocks used: Eligibility traces with a DPI (in green), Weight updates (in violet), Bistability (in red) and Comparators with WTA (in yellow). Not shown is the circuit that implements the pre-synaptic spike extension. The voltage and current variables reflect the model equation. Adapted from: Maldonado Huayaney et al. (2016).

The C-STDP rule proposed by Graupner & Brunel (2007) (see Eq. (9)) attracted the attention of circuit designer thanks to its claim to closely replicate biological findings and explain synaptic plasticity in relation to both spike timing and rate. To implement the C-STDP rule proposed by Graupner & Brunel (2007) (see Eq. (9)), Maldonado Huayaney et al. (2016) made small adaptations to the original model and proposed the circuit shown in Fig. 6. Specifically, they proposed to convert the soft bounds of the efficacy update to hard bounds, resulting in the following model for the update of the synaptic efficacy:

$$\begin{aligned} \tau \frac{d\rho}{dt} &= -k_{bs}\rho(1-\rho)(\rho_{\star} - \rho) + \gamma_p \Theta[c(t) - \theta_p] - \gamma_d \Theta[c(t) - \theta_d] \\ \rho > 1 &\rightarrow \rho = 1 \\ \rho < 0 &\rightarrow \rho = 0 \end{aligned} \quad (21)$$

with k_{bs} acting as a constant which scales the bistability dynamics and the hard-bounds implemented by the Heaviside function Θ . The building blocks implemented in this work are shown in Fig. 6. The trace block implements the local spike trace $c(t)$ represented by the voltage $V_c(t)$. It consists of a DPI with two input branches.

On the arrival of either a post-synaptic spike (*post*) or the delayed pre-synaptic spike (*pre_D*) the capacitor C_{ca} is charged by a current defined by the gain of the DPI (V_{gCa}) and $V_{C_{post}}$ or $V_{C_{pre}}$, respectively. Charging the capacitor decreases the voltage $V_c(t)$. In the absence of input pulses, the capacitor discharges at a rate controlled by $V_{\tau Ca}$ towards its resting voltage V_{cref} . The voltage $V_c(t)$ of the trace block sets the amplitude of the current $I_c(t)$ within the comparator blocks (see Fig. 6). The current $I_c(t)$ is compared with the potentiation and depression thresholds defined by the currents $I_{\theta p}$ and $I_{\theta d}$, respectively. The WTA functionality of the comparator circuits implements the Heavyside functionality of the comparison of the local spike trace $c(t)$ with the thresholds for potentiation (θ_p) and depression (θ_d) in the model (see Eq. (9)).

While the Calcium current $I_c(t)$ is greater than the potentiation threshold current $I_{\theta p}$, the synapse efficacy capacitor C_ρ within the weight update block (see Fig.6) is continuously charged by a current defined by the parameter $V_{\gamma p}$. Similarly, as long as $I_c(t)$ is greater than the depression threshold current $I_{\theta d}$, C_ρ is constantly discharged with a current controlled by $V_{\gamma d}$. The voltage across the synapse capacitor V_ρ resembles the efficacy ρ of the synapse. To implement the bistability behavior of the synaptic efficacy, Maldonado et al. use an TA in positive feedback configuration with a very small gain defined by V_b (see Fig. 6). As long as the synaptic efficacy voltage V_ρ is above the bistability threshold $V_{\rho\star}$ the positive feedback constantly charges the capacitor C_ρ and drives V_ρ towards the upper limit defined by V_{wh} . In the case that V_ρ is below $V_{\rho\star}$, the TA discharges the capacitor and drives V_ρ toward the lower limit defined by V_{wl} .

5.6. Rate Dependent Synaptic Plasticity (RDSP)

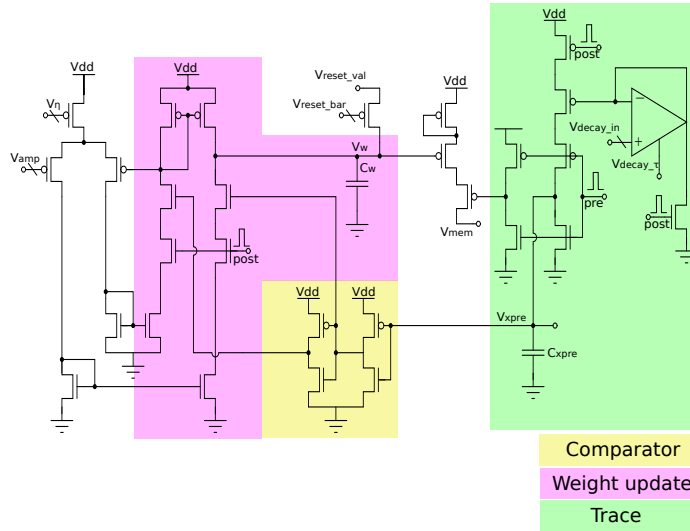


Figure 7: RDSP circuit with highlighted the CMOS building blocks used: Eligibility traces (in green), weight updates (in violet) and comparators with differential pair (in yellow). Adapted from: Häfliger et al. (1997).

The first CMOS implementation of a spike-based learning rule done by Häfliger et al. (1997) pre-dates the formalization of the RDSP model, which happened almost 20 years later (Diehl & Cook 2015). It is one of the most apparent cases of how building electronic circuits that mimic biological behavior leads to the discovery of useful mechanisms for solving real-world problems.

The algorithmic definition of their learning rule is based on a correlation signal, local to each synapse, which keeps track of the pre-synaptic spike activity. The correlation signal is refreshed at each pre-synaptic event and decays over time. When a post-synaptic spike arrives, depending on the value of the correlation, the weight is either increased or decreased, while the correlation signal is reset. Similarly, the RDSP rule relies on the pre-synaptic spike time information and is triggered when a post synaptic spike arrives. The direction of weight update depends on a target value x_{tar} , which determines the threshold between depression and potentiation.

The two main differences between the circuit by Häfliger et al. (1997) (see Fig. 7) and the RDSP rule (see Eq. (15)) is that the correlation signal in Häfliger et al. (1997) is binary and is compared to a fixed threshold voltage (the switching threshold of the first inverter), which resembles a fixed x_{tar} . In the Häfliger et al. (1997) implementation, the voltage V_w across the capacitor C_w represents the synaptic weight and the voltage V_{xpre} at the capacitor C_{xpre} represents the correlation signal. At the arrival of a pre-synaptic input spike (*pre*), the voltage V_w determines the amplitude of the current towards the soma (V_{mem}) of the post-synaptic neuron. At the same time, the capacitor C_{xpre} is fully discharged and V_{xpre} is low. In the absence of pre-synaptic and post-synaptic spikes (*pre* and *post* are low), C_{xpre} is slowly charged towards V_{dd} by the pMOS branch in the trace block (see Fig. 7).

The voltage V_{xpre} is constantly compared to the threshold voltage (resembling x_{tar}) of the first inverter it is connected to. At the arrival of a post-synaptic spike (*post* is high) the weight capacitor C_w is either charged (depressed) or discharged (potentiated) depending on the momentary level of V_{xpre} . If V_{xpre} is above the inverter threshold voltage, the right branch of the weight update block (see Fig. 7) is inactive, while the left branch is active and the pMOS-based current mirror charges the capacitor C_w . In the opposite case, where V_{xpre} is below the inverter threshold voltage, the right branch is active while the output of the second inverter disables the left branch of the weight update block. This results in a discharge of the capacitor C_w controlled by the nMOS-based current mirror. The amplitude for potentiation and depression is set by the two biases V_η and V_{amp} . At the end of a post-synaptic spike the correlation signal V_{xpre} is reset to V_{dd} . A similar approach implementing a nearest-spike interaction scheme and a fixed x_{tar} was implemented by Ramakrishnan et al. (2011) exploiting the properties of floating gates.

5.7. Other models implementations

To the best of our knowledge, there have been no dedicated CMOS-based implementations of the other models presented in Sec. 4. Although the V-STDP rule proposed by Clopath et al. (2010) and Clopath & Gerstner (2010) shares similarities with the T-STDP rule and can be related to the BCM rule (Gjorgjieva et al. 2011), its complexity for implementations comes from its multiple transient signals on different timescales. To this end, emerging novel technologies, such as memristors (Cantley et al. 2011, Li et al. 2013, Li et al. 2014, Ziegler et al. 2015, Diederich et al. 2018) and neuristors (John et al. 2018) are capable of supporting promising solutions

to implement different timescales in a compact and efficient manner. Similarly, implementations for the DPSS rule (Urbanczik & Senn 2014) are difficult due to the increased complexity of the required multi-compartment neuron models. Recently, implementations based on hybrid memristor-CMOS systems (Nair et al. 2017, Payvand et al. 2020) or using existing neuromorphic processors to exploit neuron structures to replicate the multi-compartment model (Cartiglia et al. 2020) have been proposed. A detailed view on these implementations is beyond the scope of this review and the authors refer the readers to the original publications.

However, introducing CMOS implemented models through the lens of functional building blocks allows us to quickly look for analogies and differences between the implemented and other models. Throughout this Section, we have highlighted the similarities and differences of each of the implemented models. Focusing on functional building blocks also allows for a broader generalization to all the models that have not been implemented yet: using the basic building block we presented (e.g. Traces, Comparators, Weight updates, and Bistability) one could potentially construct all the learning models we have discussed in Sec. 4.

6. Discussion and conclusion

6.1. Toward a unified synaptic plasticity framework

In this survey, we highlighted the similarities and differences of representative synaptic plasticity models and provided examples of neuromorphic circuits CMOS that can be used to implement their principles of computation. We highlighted how the principle of locality in learning and neural computation in general is fundamental and enables the development of fast, efficient and scalable neuromorphic processing systems. We highlighted how the different features of the plasticity models can be summarized in (1) synaptic weights properties, (2) plasticity update triggers and (3) local variables that can be exploited to modify the synaptic weight (see also Table 1). Although all local variables of these rules are similar in nature, the plasticity rules can be subdivided in the following way:

- Pre-synaptic spike trace: RDSP.
- Pre- and post-synaptic spike traces: STDP, T-STDP, C-STDP, SBCM, BDSP.
- Pre-synaptic spike trace + post-synaptic membrane voltage: V-STDP, DPSS, MPDP, H-MPDP.
- Post-synaptic membrane voltage + post-synaptic spike trace: SDSP, C-MPDP.

Many possibilities arise when exploring how the local variables used by these rules interact (e.g. comparison, addition, multiplication, etc.). This leads to a wide range of additional models that could be proposed and to a large number of biological experiments that could be carried out to verify the hypotheses and predictions made by the rules.

It is difficult to predict whether a unified rule of synaptic plasticity can be formulated, based on the observation that several plasticity mechanisms coexist in the brain (Abbott & Nelson 2000, Bi & Poo 2001), and that different problems may require different plasticity mechanisms. Nevertheless, we provided here a single unified framework that allowed us to do a systematic comparison of the features of many representative models of synaptic plasticity presented in the literature, developed

following experiment-driven bottom-up approaches and/or application-driven top-down approaches (Frenkel et al. 2021). While the bottom-up approach can help in explaining the plasticity mechanisms found in the brain, top-down guidance can help to find the right level of abstraction from biology to get the best performance for solving problems in the context of efficient and adaptive artificial systems. In line with the neuromorphic engineering perspective, this work bridges the gap between both approaches.

6.2. Overcoming back-propagation limits for online learning

Local synaptic plasticity in neuromorphic circuits offers a promising solution for online learning in embedded systems. However, due to the very local nature of this approach, there is no direct way of implementing global learning rules in multi-layer neural networks, such as the gradient-based back-propagation algorithm (LeCun et al. 1998, Schmidhuber et al. 2007). This algorithm has been the work horse of ANNs training in deep learning over the last decade. Gradient-based learning has recently been applied for offline training of SNNs, where the Back-Propagation (BP) algorithm coupled with surrogate gradients is used to solve two critical problems: first, the temporal credit assignment problem which arises due to the temporal inter-dependencies of the SNN activity. It is solved offline with Back-Propagation Through Time (BPTT) by unrolling the SNN like standard Recurrent Neural Networks (RNNs) (Neftci et al. 2019). Second, the spatial credit assignment problem, where the credit or “blame” with respect to the objective function is assigned to each neuron across the layers. However, BPTT is not biologically plausible (Bengio et al. 2015, Lillicrap et al. 2020) and not practical for on-chip and online learning due to the non-local learning paradigm. On one hand, BPTT is not local in time as it requires keeping all the network activities for the duration of the trial. On the other hand, BPTT is not local in space as it requires information to be transferred across multiple layers. Indeed, synaptic weights can only be updated after complete forward propagation, loss evaluation, and back-propagation of error signals, which lead to the so-called “locking effect” (Czarnecki et al. 2017).

Recently, intensive research in neuromorphic computing has been dedicated to bridge the gap between back-propagation and local synaptic plasticity rules by reducing the non-local information requirements, at a cost of accuracy in complex problems (Eshraghian et al. 2021). The temporal credit assignment can be handled by using eligibility traces (Zenke & Ganguli 2018, Bellec et al. 2020) that solve the distal reward problem by bridging the delay between the network output and the feedback signal that may arrive later in time (Izhikevich 2007). Similarly, inspired by recent progress in deep learning, several strategies have been explored to solve the spatial credit assignment problem using feedback alignment (Lillicrap et al. 2016), direct feedback alignment (Nøkland 2016), random error BP (Neftci et al. 2017) or by replacing the backward pass with an additional forward pass whose input is modulated with error information (Dellafrera & Kreiman 2022). However, these approaches only partially solve the problem (Eshraghian et al. 2021), since they still suffer from the locking effect, which can nonetheless be tackled by replacing the global loss by a number of local loss functions (Mostafa et al. 2018, Neftci et al. 2019, Kaiser et al. 2020, Halvagal & Zenke 2022) or by using direct random target projection (Frenkel et al. 2021). Assigning credit locally, especially within recurrent SNNs, is still an open question and an active field of research (Christensen

et al. 2021).

The local synaptic plasticity models and circuits presented in this survey do not require the presence of a teacher signal and contrast with supervised learning using labeled data which is neither biologically plausible (Halvagal & Zenke 2022) nor practical in most online scenarios (Muliukov et al. 2022). Nevertheless, the main limit of spike-based local learning is the diminished performance on complex pattern recognition problems. Different approaches have been explored to bridge this gap, such as DPSS (Urbanczik & Senn 2014, Sacramento et al. 2018) and BDSP (Payeur et al. 2021) learning rules that use multi-compartment neurons and show promising performance in approximating back-propagation with local mechanisms, or using multi-modal association to improve the self-organizing system’s performance (Gilra & Gerstner 2017, Khacef et al. 2020a, Rathi & Roy 2021) as in contrast to labeled data, multiple sensory modalities (e.g. sight, sound, touch) are freely available in the real-world environment.

6.3. Structural plasticity and network topology

Exploring local synaptic plasticity rules gives valuable insights into how plasticity and learning evolves in the brain. However, in bringing the plasticity of single synapses to the function of entire networks, many more factors come into play. Functionality at a network level is determined by the interplay between the synaptic learning rules, the spatial location of the synapse, and the neural network topology.

Furthermore, the network topology of the brain is itself plastic (Holtmaat & Svoboda 2009). Le Bé & Markram (2006) provided the first direct demonstration of induced rewiring (i.e. sprouting and pruning) of a functional circuit in the neocortex (Markram et al. 2011), which requires hours of general stimulation. Some studies suggest that glutamate release is a key determinant in synapse formation (Engert & Bonhoeffer 1999, Kwon & Sabatini 2011), but additional investigations are needed to better understand the computational foundations of structural plasticity and how it is linked to the synaptic plasticity models we reviewed in this survey. Together, structural and synaptic plasticity are the local mechanisms that lead to the emergence of the global structure and function of the brain. Understanding, modeling, and implementing the interplay between these two forms of plasticity is a key challenge for the design of self-organizing systems that can get closer to the unique efficiency and adaptation capabilities of the brain.

6.4. CMOS neuromorphic circuits

The computational primitives that are shared by the different plasticity models were grouped together in corresponding functional primitives and circuit blocks that can be combined to map multiple plasticity models into corresponding spike-based learning circuits. Many of the models considered rely on exponentially decaying traces. By operating the CMOS circuits in the sub-threshold regime, this exponential dependency is given by the physical substrate of transistors showing an exponential relationship between current and voltage (Mead 1990).

The circuits presented make use of both analog computation (e.g. analog weight updates) and digital communication (e.g. pre- and post-synaptic spike events). This mixed-signal analog/digital approach aligns with the observations that biological neural systems can be considered as hybrid analog and digital processing

systems (Sarpeshkar 1998). Due to the digital nature of spike transmission in these neuromorphic systems, plasticity circuits that require the use of pre-synaptic traces need extra overhead to generate this information directly at the post-synaptic side.

The emergence of novel nanoscale memristive devices has high potential for allowing the implementation of such circuits at a low overhead cost, in terms of space and power (Demirag et al. 2021). In addition, these emerging memory technologies have the potential of allowing long-term storage of the synaptic weights in a non-volatile way, that would allow these neuromorphic systems to operate continuously, without having to upload the neural network parameters at boot time. This will be a significant advantage in large-scale systems, as Input/Output operations required to load network parameters can take a significant amount of power and time. In addition, the properties of emerging memristive devices could be exploited to implement different features of the plasticity models proposed (Diederich et al. 2018).

Overall, the number of proposed CMOS-based analog or mixed-signal neuromorphic circuits over the past 25 years is relatively low, as this was mainly driven by fundamental academic research. With the increasing need for low-power neural processing systems at the edge, the increasing maturity of novel technologies, and the rising interest in brain-inspired neural networks and learning for data processing, we can expect an increasing number of new mixed signal analog/digital circuits implementing new plasticity rules also for commercial exploitation. In this respect, this review can provide valuable information for making informed modeling and circuit design decision in developing novel spike-based neuromorphic processing systems for online learning.

Acknowledgments

We would like to thank the BICS group for the fruitful discussions, with a special thank to Hugh Greatorrex for providing valuable comments on the manuscript. We would also like to acknowledge the financial support of the CogniGron research center and the Ubbo Emmius Funds of the University of Groningen, the European Union's H2020 research and innovation programme under the H2020 BeFerro synaptic project (871737), the Swiss National Science Foundation Sinergia project (CRSII5-18O316) and the ERC grant NeuroAgents (724295).

Data availability statement

No new data were created or analyzed in this study.

ORCID IDs

Lyes Khacef: <https://orcid.org/0000-0002-4009-174X>.

Philipp Klein: <https://orcid.org/0000-0003-4266-2590>.

Matteo Cartiglia: <https://orcid.org/0000-0001-8936-6727>.

Arianna Rubino: <https://orcid.org/0000-0002-5036-1969>.

Giacomo Indiveri: <https://orcid.org/0000-0002-7109-1689>.

Elisabetta Chicca: <https://orcid.org/0000-0002-5518-8990>.

References

- Abbott, L. & Nelson, S. (2000). Synaptic plasticity: taming the beast, *Nature Neuroscience* **3**: 1178–1183.
- Abbott, L. & Song, S. (1999). Asymmetric hebbian learning, spike timing and neural response variability, *Advances in Neural Information Processing Systems*, Vol. 11, pp. 69–75.
- Albers, C., Westkott, M. & Pawelzik, K. (2016). Learning of precise spike times with homeostatic membrane potential dependent synaptic plasticity, *PLOS ONE* **11**(2): 1–28.
- Arthur, J. & Boahen, K. (2006). Learning in silicon: Timing is everything, in Y. Weiss, B. Schölkopf & J. Platt (eds), *Advances in Neural Information Processing Systems 18*, MIT Press, Cambridge, MA.
- Artola, A., Bröcher, S. & Singer, W. (1990). Different voltage-dependent thresholds for inducing long-term depression and long-term potentiation in slices of rat visual cortex, *Nature* **347**: 69–72.
- Azghadi, M. R., Al-Sarawi, S., Abbott, D. & Iannella, N. (2013). A neuromorphic VLSI design for spike timing and rate based synaptic plasticity, *Neural Networks* **45**: 70–82.
- Bain, A. (1873). Mind and body: the theories of their relation, New York: D. Appleton and company.
- Bamford, S. A., Murray, A. F. & Willshaw, D. J. (2012). Spike-timing-dependent plasticity with weight dependence evoked from physical constraints, *IEEE Transactions on Biomedical Circuits and Systems* **6**(4): 385–398.
- Bartol, Thomas M, J., Bromer, C., Kinney, J., Chirillo, M. A., Bourne, J. N., Harris, K. M. & Sejnowski, T. J. (2015). Nanoconnectomic upper bound on the variability of synaptic plasticity, *eLife* **4**: e10778.
URL: <https://doi.org/10.7554/eLife.10778>
- Bekolay, T., Kolbeck, C. & Eliasmith, C. (2013). Simultaneous unsupervised and supervised learning of cognitive functions in biologically plausible spiking neural networks, *Cognitive Science* **35**.
- Bellec, G., Scherr, F., Subramoney, A., Hajek, E., Salaj, D., Legenstein, R. & Maass, W. (2020). A solution to the learning dilemma for recurrent networks of spiking neurons, *Nature Communications* **11**.
- Bengio, Y., Lee, D. H., Bornschein, J. & Lin, Z. (2015). Towards biologically plausible deep learning, *ArXiv abs/1502.04156*.
- Bi, G. Q. & Poo, M. M. (1998). Synaptic modifications in cultured hippocampal neurons: dependence on spike timing, synaptic strength, and postsynaptic cell type, *The Journal of Neuroscience* **18**(24): 10464–10472.
- Bi, G. Q. & Poo, M. M. (2001). Synaptic modification by correlated activity: Hebb’s postulate revisited, *Annual Review of Neuroscience* **24**(1): 139–166.
- Bichler, O., Querlioz, D., Thorpe, S. J., Bourgoin, J. P. & Gamrat, C. (2012). Extraction of temporally correlated features from dynamic vision sensors with spike-timing-dependent plasticity, *Neural Networks* **32**: 339–348.
- Bienenstock, E., Cooper, L. & Munro, P. (1982). Theory for the development of neuron selectivity: orientation specificity and binocular interaction in visual cortex, *Jour. Neurosci.* **2**(1): 32–48.
URL: <http://www.jneurosci.org/cgi/content/abstract/2/1/32>
- Binas, J., Indiveri, G. & Pfeiffer, M. (2015). Local structure helps learning optimized automata in recurrent neural networks, *International Joint Conference on Neural Networks, (IJCNN)*, IEEE, pp. 1–7.
- Biology of Synaptic Plasticity* (2020). [Online; accessed 2021-08-05].
- Bliss, T. P. & Collingridge, G. (1993). A synaptic model of memory: Long term potentiation in the hippocampus, *Nature* **31**: 361.
- Bofill-i-Petit, A. & Murray, A. (2004). Synchrony detection and amplification by silicon neurons with STDP synapses, *IEEE Transactions on Neural Networks* **15**(5): 1296–1304.
- Bofill-i-Petit, A., Thompson, D. & Murray, A. (2001). Circuits for VLSI implementation of temporally asymmetric Hebbian learning, in T. Dietterich, S. Becker & Z. Ghahramani (eds), *Advances in Neural Information processing systems*, Vol. 14, MIT Press, Cambridge, MA.
- Bourne, J. N., Chirillo, M. A. & Harris, K. M. (2013). Presynaptic ultrastructural plasticity along ca3→ca1 axons during long-term potentiation in mature hippocampus, *Journal of Comparative Neurology* **521**(17): 3898–3912.
URL: <https://onlinelibrary.wiley.com/doi/abs/10.1002/cne.23384>
- Brader, J., Senn, W. & Fusi, S. (2007). Learning real world stimuli in a neural network with spike-driven synaptic dynamics, *Neural Computation* **19**: 2881–2912.
- Branco, T., Staras, K., Darcy, K. J. & Goda, Y. (2008). Local dendritic activity sets release probability at hippocampal synapses, *Neuron* **59**(3): 475–485.
URL: <https://www.sciencedirect.com/science/article/pii/S089662730800576X>

- Brette, R. (2015). Philosophy of the spike: Rate-based vs. spike-based theories of the brain, *Frontiers in Systems Neuroscience* **9**(151): 1–14.
- Cameron, K., Boonsobhak, V., Murray, A. & Renshaw, D. (2005). Spike timing dependent plasticity (stdp) can ameliorate process variations in neuromorphic vlsi, *IEEE Transactions on Neural Networks* **16**(6): 1626–1637.
- Cantley, K. D., Subramaniam, A., Stiegler, H. J., Chapman, R. A. & Vogel, E. M. (2011). Spike timing-dependent synaptic plasticity using memristors and nano-crystalline silicon tft memories, *2011 11th IEEE International Conference on Nanotechnology*, pp. 421–425.
- Cartiglia, M., Haessig, G. & Indiveri, G. (2020). An error-propagation spiking neural network compatible with neuromorphic processors, *2020 2nd IEEE International Conference on Artificial Intelligence Circuits and Systems (AICAS)*.
- Chang, C.-C., Chen, P.-C., Hudec, B., Liu, P.-T. & Hou, T.-H. (2018). Interchangeable hebbian and anti-hebbian stdp applied to supervised learning in spiking neural network, *2018 IEEE International Electron Devices Meeting (IEDM)*, pp. 15.5.1–15.5.4.
- Chen, Y. (2017). Mechanisms of winner-take-all and group selection in neuronal spiking networks, *Frontiers in Computational Neuroscience* **11**.
URL: <https://www.frontiersin.org/article/10.3389/fncom.2017.00020>
- Chicca, E., Badoni, D., Dante, V., D’Andreagiovanni, M., Salina, G., Carota, L., Fusi, S. & Del Giudice, P. (2003). A VLSI recurrent network of integrate-and-fire neurons connected by plastic synapses with long-term memory, *IEEE Transactions on Neural Networks* **14**(5): 1297–1307.
- Chicca, E. & Fusi, S. (2001). Stochastic synaptic plasticity in deterministic aVLSI networks of spiking neurons, in F. Rattay (ed.), *Proceedings of the World Congress on Neuroinformatics*, ARGESIM Reports, ARGESIM/ASIM Verlag, Vienna, Austria, pp. 468–477.
- Chicca, E., Stefanini, F., Bartolozzi, C. & Indiveri, G. (2014). Neuromorphic electronic circuits for building autonomous cognitive systems, *Proceedings of the IEEE* **102**(9): 1367–1388.
- Chindemi, G., Abdellah, M., Amsalem, O., Benavides-Piccione, R., Delattre, V., Doron, M., Ecker, A., Jaquier, A. T., King, J., Kumbhar, P., Monney, C., Perin, R., Rössert, C., Tuncel, A. M., Geit, W., DeFelipe, J., Graupner, M., Segev, I., Markram, H. & Muller, E. B. (2022). A calcium-based plasticity model for predicting long-term potentiation and depression in the neocortex, *Nature Communications* **13**(1): 1–19.
- Christensen, D. V., Dittmann, R., Linares-Barranco, B., Sebastian, A., Le Gallo, M., Redaelli, A., Slesazeck, S., Mikolajick, T., Spiga, S., Menzel, S., Valov, I., Milano, G., Ricciardi, C., Liang, S. J., Miao, F., Lanza, M., Quill, T. J., Keene, S. T., Salleo, A., Grollier, J., Markovic, D., Mizrahi, A., Yao, P., Yang, J. J., Indiveri, G., Strachan, J. P., Datta, S., Vianello, E., Valentian, A., Feldmann, J., Li, X., Pernice, W. H. P., Bhaskaran, H., Neftci, E., Ramaswamy, S., Tapson, J., Scherr, F., Maass, W., Panda, P., Kim, Y., Tanaka, G., Thorpe, S., Bartolozzi, C., Cleland, T. A., Posch, C., Liu, S. C., Mazumder, A. N., Hosseini, M., Mohsenin, T., Donati, E., Tolu, S., Galeazzi, R., Christensen, M. E., Holm, S., Ielmini, D. & Pryds, N. (2021). 2021 roadmap on neuromorphic computing and engineering.
- Clopath, C., Büsing, L., Vasilaki, E. & Gerstner, W. (2010). Connectivity reflects coding: a model of voltage-based STDP with homeostasis, *Nature Neuroscience* **13**(3): 344–352.
- Clopath, C. & Gerstner, W. (2010). Voltage and spike timing interact in stdp – a unified model, *Frontiers in Synaptic Neuroscience* **2**: 25.
- Czarnecki, W. M., Swirszcz, G., Jaderberg, M., Osindero, S., o. Vinyals & Kavukcuoglu, K. (2017). Understanding synthetic gradients and decoupled neural interfaces, *Proceedings of the 34th International Conference on Machine Learning - Volume 70*, ICML’17, JMLR.org, p. 904–912.
- Dante, V., del giudice, P. & Mattia, M. (2001). Implementation of neuromorphic systems: from discrete components to analog vlsi chips (testing and communication issues), *Annali dell’Istituto superiore di sanità* **37**: 231–9.
- Dayan, P. & Abbott, L. (2001). *Theoretical Neuroscience: Computational and Mathematical Modeling of Neural Systems*, MIT Press.
- Del Giudice, P., Fusi, S. & Mattia, M. (2003). Modeling the formation of working memory with networks of integrate-and-fire neurons connected by plastic synapses, *Journal of Physiology Paris* **97** pp. 659–681.
- Dellafrera, G. & Kreiman, G. (2022). Error-driven input modulation: Solving the credit assignment problem without a backward pass, *CoRR* **abs/2201.11665**.
URL: <https://arxiv.org/abs/2201.11665>
- Demirag, Y., Moro, F., Dalgaty, T., Navarro, G., Frenkel, C., Indiveri, G., Vianello, E. & Payvand, M. (2021). PCM-trace: Scalable synaptic eligibility traces with resistivity drift of phase-change

- materials, *International Symposium on Circuits and Systems, (ISCAS)*, IEEE, pp. 1–5.
- DeWolf, T., Jaworski, P. & Eliasmith, C. (2020). Nengo and low-power ai hardware for robust, embedded neurorobotics, *Frontiers in Neurobotics* **14**: 73.
- Diederich, N., Bartsch, T., Kohlstedt, H. & Ziegler, M. (2018). A memristive plasticity model of voltage-based stdp suitable for recurrent bidirectional neural networks in the hippocampus, *Scientific Reports* **8**(1).
- Diehl, P. & Cook, M. (2015). Unsupervised learning of digit recognition using spike-timing-dependent plasticity, *Frontiers in Computational Neuroscience* **9**: 99.
- Engert, F. & Bonhoeffer, T. (1999). Dendritic spine changes associated with hippocampal long-term synaptic plasticity, *Nature* **399**: 66–70.
- Eshraghian, J. K., Ward, M., Neftci, E., Wang, X., Lenz, G., Dwivedi, G., Bennamoun, M., Jeong, D. S. & Lu, W. D. (2021). Training spiking neural networks using lessons from deep learning.
- French, R. M. (1999). Catastrophic forgetting in connectionist networks, *Trends in Cognitive Sciences* **3**(4): 128–135.
- Frenkel, C., Bol, D. & Indiveri, G. (2021). Bottom-up and top-down neural processing systems design: Neuromorphic intelligence as the convergence of natural and artificial intelligence.
- Fusi, S., Annunziato, M., Badoni, D., Salamon, A. & Amit, D. J. (2000). Spike-driven synaptic plasticity: Theory, simulation, VLSI implementation, *Neural Computation* **12**: 2227–2258.
- Fusi, S., Del Giudice, P. & Amit, D. (2000). Neurophysiology of a vlsi spiking neural network: Lann21, *Proceedings of the IEEE-INNS-ENNS International Joint Conference on Neural Networks. IJCNN 2000. Neural Computing: New Challenges and Perspectives for the New Millennium*, Vol. 3, pp. 121–126 vol.3.
- Fusi, S., Drew, P. & Abbott, L. (2005). Cascade models of synaptically stored memories, *Neuron* **45**: 599–611.
- Gerstner, W., Lehmann, M., Liakoni, V., Corneil, D. & Brea, J. (2018). Eligibility traces and plasticity on behavioral time scales: Experimental support of neohebbian three-factor learning rules, *Frontiers in Neural Circuits* **12**: 53.
- Gerstner, W., Ritz, R. & van Hemmen, J. L. (1993). Why spikes? hebbian learning and retrieval of time-resolved excitation patterns, *Biological cybernetics* **69**(5-6): 503–515.
- Gilra, A. & Gerstner, W. (2017). Predicting non-linear dynamics by stable local learning in a recurrent spiking neural network, *eLife* **6**: 1–43.
- Giulioni, M., Camilleri, P., Dante, V., Badoni, D., Indiveri, G., Braun, J. & Del Giudice, P. (2008). A VLSI network of spiking neurons with plastic fully configurable “stop-learning” synapses, *International Conference on Electronics, Circuits, and Systems, ICECS 2008*, IEEE, pp. 678–681.
- Gjorgjieva, J., Clopath, C., Audet, J. & Pfister, J. P. (2011). A triplet spike-timing-dependent plasticity model generalizes the bienenstock-cooper-munro rule to higher-order spatiotemporal correlations, *Proceedings of the National Academy of Sciences* **108**(48): 19383–19388.
- Gopalakrishnan, R. & Basu, A. (2014). Robust doublet STDP in a floating-gate synapse, *2014 International Joint Conference on Neural Networks (IJCNN)*, pp. 4296–4301.
- Gopalakrishnan, R. & Basu, A. (2017). Triplet spike time-dependent plasticity in a floating-gate synapse, *IEEE Transactions on Neural Networks and Learning Systems* **28**(4): 778–790.
- Graupner, M. & Brunel, N. (2007). Stdp in a bistable synapse model based on CaMKII and associated signaling pathways, *PLOS Computational Biology* **3**(11): 2299–2323.
- Graupner, M. & Brunel, N. (2010). Mechanisms of induction and maintenance of spike-timing dependent plasticity in biophysical synapse models, *Frontiers in Computational Neuroscience* **4**(136): 1–19.
- Graupner, M. & Brunel, N. (2012). Calcium-based plasticity model explains sensitivity of synaptic changes to spike pattern, rate, and dendritic location, *Proceedings of the National Academy of Sciences* **109**(10): 3991–3996.
- Häfliger, P., Mahowald, M. & Watts, L. (1997). A spike based learning neuron in analog VLSI, in M. Mozer, M. Jordan & T. Petsche (eds), *Advances in neural information processing systems*, Vol. 9, MIT Press, pp. 692–698.
- Halvagal, M. S. & Zenke, F. (2022). The combination of hebbian and predictive plasticity learns invariant object representations in deep sensory networks.
URL: <https://doi.org/10.1101/2022.03.17.484712>
- Harris, K. & Stevens, J. (1989). Dendritic spines of ca 1 pyramidal cells in the rat hippocampus: serial electron microscopy with reference to their biophysical characteristics, *Journal of Neuroscience* **9**(8): 2982–2997.
URL: <https://www.jneurosci.org/content/9/8/2982>
- Harris, K. & Sultan, P. (1995). Variation in the number, location and size of synaptic vesicles provides

- an anatomical basis for the nonuniform probability of release at hippocampal cal synapses, *Neuropharmacology* **34**(11): 1387–1395.
URL: <https://www.sciencedirect.com/science/article/pii/002839089500142S>
- Hawkins, J., Ahmad, S. & Cui, Y. (2017). A theory of how columns in the neocortex enable learning the structure of the world, *Frontiers in Neural Circuits* **11**.
URL: <https://www.frontiersin.org/articles/10.3389/fncir.2017.00081>
- Hazan, H., Saunders, D., Sanghavi, D. T., Siegelmann, H. & Kozma, R. (2018). Unsupervised learning with self-organizing spiking neural networks, *2018 International Joint Conference on Neural Networks (IJCNN)*, pp. 1–6.
- Hebb, D. O. (1949). *The organization of behavior: a neuropsychological theory*, Taylor & Francis, 2012.
- Hering, H. & Sheng, M. (2001). Dendritic spines: structure, dynamics and regulation, *Nature Reviews Neuroscience*.
- Ho, V. M., Lee, J.-A. & Martin, K. C. (2011). The cell biology of synaptic plasticity, *Science* **334**(6056): 623–628.
URL: <https://www.science.org/doi/abs/10.1126/science.1209236>
- Hofman, M. A. (2015). Evolution of the human brain: From matter to mind, pp. 65–82.
- Holtmaat, A. & Svoboda, K. (2009). Experience-dependent structural synaptic plasticity in the mammalian brain, *Nature Reviews Neuroscience* **10**: 647–58.
- Hyvärinen, A. & Oja, E. (2000). Independent component analysis: algorithms and applications, *Neural Networks* **13**(4): 411–430.
URL: <https://www.sciencedirect.com/science/article/pii/S0893608000000265>
- Indiveri, G. (2002). Neuromorphic bistable VLSI synapses with spike-timing-dependent plasticity, *Advances in Neural Information Processing Systems*, Vol. 15, MIT Press, Cambridge, MA, pp. 1091–1098.
- Indiveri, G. (2003). Neuromorphic selective attention systems, *International Symposium on Circuits and Systems, ISCAS 2003, IEEE*, pp. III–770–III–773.
- Indiveri, G., Chicca, E. & Douglas, R. J. (2006). A VLSI array of low-power spiking neurons and bistable synapses with spike-timing dependent plasticity, *IEEE Transactions on Neural Networks* **17**(1): 211–221.
URL: http://ncs.ethz.ch/pubs/pdf/Indiveri_et.al06.pdf
- Iyer, L. R. & Basu, A. (2017). Unsupervised learning of event-based image recordings using spike-timing-dependent plasticity, *2017 International Joint Conference on Neural Networks (IJCNN)*, pp. 1840–1846.
- Izhikevich, E. (2007). Solving the distal reward problem through linkage of STDP and dopamine signaling, *Cereb. Cortex*. In press.
- James, W. (1890). *The principles of psychology*, New York: Henry Holt and Company.
- John, R. A., Liu, F., Chien, N. A., Kulkarni, M. R., Zhu, C., Fu, Q., Basu, A., Liu, Z. & Mathews, N. (2018). Synergistic gating of electro-iono-photoactive 2d chalcogenide neuristors: Coexistence of hebbian and homeostatic synaptic metaplasticity, *Advanced Materials* **30**(25): 1800220.
- Kaiser, J., Mostafa, H. & Neftci, E. (2020). Synaptic plasticity dynamics for deep continuous local learning (decolle), *Frontiers in Neuroscience* **14**: 424.
- Karmarkar, U. R. & Buonomano, D. V. (2002). A model of spike-timing dependent plasticity: One or two coincidence detectors?, *Journal of Neurophysiology* **88**(1): 507–513.
- Khacef, L., Rodriguez, L. & Miramond, B. (2020a). Brain-inspired self-organization with cellular neuromorphic computing for multimodal unsupervised learning, *Electronics* **9**(10).
- Khacef, L., Rodriguez, L. & Miramond, B. (2020b). Improving self-organizing maps with unsupervised feature extraction, *Neural Information Processing*, Springer International Publishing, Cham, pp. 474–486.
- Kheradpisheh, S. R., Ganjtabesh, M., Thorpe, S. J. & Masquelier, T. (2018). Stdp-based spiking deep convolutional neural networks for object recognition, *Neural Networks* **99**: 56–67.
- Kohonen, T. (1990). The self-organizing map, *Proceedings of the IEEE* **78**(9): 1464–1480.
- Koickal, T., Hamilton, A., Tan, S., Covington, J., Gardner, J. & Pearce, T. (2007). Analog vlsi circuit implementation of an adaptive neuromorphic olfaction chip, *IEEE Transactions on Circuits and Systems I: Regular Papers* **54**: 60–73.
- Kwon, H. B. & Sabatini, B. L. (2011). Glutamate induces de novo growth of functional spines in developing cortex, *Nature* **474**: 100 – 104.
- Lalée, S. & Dominey, P. F. (2013). Multi-modal convergence maps: from body schema and self-representation to mental imagery, *Adaptive Behavior* **21**(4): 274–285.
- Le Bé, J. V. & Markram, H. (2006). Spontaneous and evoked synaptic rewiring in the neonatal neocortex, *Proceedings of the National Academy of Sciences of the United States of America*

- 103:** 13214–9.
- LeCun, Y., Bottou, L., Bengio, Y. & Haffner, P. (1998). Gradient-based learning applied to document recognition, *Proceedings of the IEEE* **86**(11): 2278–2324.
- Li, Y., Zhong, Y., Xu, L., Zhang, J., Xu, X., Sun, H. & Miao, X. (2013). Ultrafast synaptic events in a chalcogenide memristor, *Scientific Reports* **3**(1).
- Li, Y., Zhong, Y., Zhang, J., Xu, L., Wang, Q., Sun, H., Tong, H., Cheng, X. & Miao, X. (2014). Activity-dependent synaptic plasticity of a chalcogenide electronic synapse for neuromorphic systems, *Scientific Reports* **4**(1).
- Lillicrap, T. P., Cownden, D., Tweed, D. B. & Akerman, C. (2016). Random synaptic feedback weights support error backpropagation for deep learning, *Nature Communications* **7**(13276): 1–10.
- Lillicrap, T. P., Santoro, A., Marris, L., Akerman, C. J. & Hinton, G. (2020). Backpropagation and the brain, *Nature Reviews Neuroscience* **21**: 335–346.
- Lisman, J. & Harris, K. (1994). Who's been nibbling on my psd: Is it ltd?, *Journal of Physiology-Paris* **88**(3): 193–195.
URL: <https://www.sciencedirect.com/science/article/pii/0928425794900051>
- Lisman, J. & Spruston, N. (2005). Postsynaptic depolarization requirements for ltp and ltd: a critique of spike timing-dependent plasticity, *Nature Neuroscience* **8**(7): 839–841.
- Lisman, J. & Spruston, N. (2010). Questions about stdp as a general model of synaptic plasticity, *Frontiers in Synaptic Neuroscience* **2**.
URL: <https://www.frontiersin.org/article/10.3389/fnsyn.2010.00140>
- Liu, S. C. & Mockel, R. (2008). Temporally learning floating-gate vlsi synapses, *2008 IEEE International Symposium on Circuits and Systems*, pp. 2154–2157.
- Locke, J. (1689). An essay concerning human understanding, W. Dennis (Ed.), Century psychology series. Readings in the history of psychology (p. 55–68). Appleton-Century-Crofts.
- Maldonado Huayaney, F. L., Nease, S. & Chicca, E. (2016). Learning in silicon beyond STDP: a neuromorphic implementation of multi-factor synaptic plasticity with calcium-based dynamics, *IEEE Transactions on Circuits and Systems I: Regular Papers* **63**(12): 2189–2199.
- Markram, H., Gerstner, W. & Sjöström, P. J. (2011). A history of spike-timing-dependent plasticity, *Frontiers in Synaptic Neuroscience* **3**(4): 1–24.
- Markram, H., Helm, P. J. & Sakmann, B. (1995). Dendritic calcium transients evoked by single back-propagating action potentials in rat neocortical pyramidal neurons, *The Journal of physiology* **485** (Pt 1): 1–20.
- Markram, H., Lübke, J., Frotscher, M. & Sakmann, B. (1997). Regulation of synaptic efficacy by coincidence of postsynaptic APs and EPSPs, *Science* **275**: 213–215.
- Mastella, M., Toso, F., Sciortino, G., Prati, E. & Ferrari, G. (2020). Tunneling-based cmos floating gate synapse for low power spike timing dependent plasticity, *2020 2nd IEEE International Conference on Artificial Intelligence Circuits and Systems (AICAS)*.
- Mayr, C., Noack, M., Partzsch, J. & Schüffny, R. (2010). Replicating experimental spike and rate based neural learning in cmos, *Proceedings of 2010 IEEE International Symposium on Circuits and Systems*, pp. 105–108.
- McNaughton, B. L., Douglas, R. M. & Goddard, G. V. (1978). Synaptic enhancement in fascia dentata: Cooperativity among coactive afferents, *Brain Research* **157**(2): 277–293.
- Mead, C. (1990). Neuromorphic electronic systems, *Proceedings of the IEEE* **78**(10): 1629–1636.
- Meng, Y., Zhou, K., Monzon, J. J. C. & Poon, C. S. (2011). Iono-neuromorphic implementation of spike-timing-dependent synaptic plasticity, *2011 Annual International Conference of the IEEE Engineering in Medicine and Biology Society*, pp. 7274–7277.
- Mitra, S., Fusi, S. & Indiveri, G. (2009). Real-time classification of complex patterns using spike-based learning in neuromorphic VLSI, *IEEE Transactions on Biomedical Circuits and Systems* **3**(1): 32–42.
- Morrison, A., Diesmann, M. & Gerstner, W. (2008). Phenomenological models of synaptic plasticity based on spike timing, *Biological Cybernetics* **98**: 459–478.
- Mostafa, H., Ramesh, V. & Cauwenberghs, G. (2018). Deep supervised learning using local errors, *Frontiers in Neuroscience* **12**: 608.
- Muliukov, A. R., Rodriguez, L., Miramond, B., Khacef, L., Schmidt, J., Berthet, Q. & Upegui, A. (2022). A unified software/hardware scalable architecture for brain-inspired computing based on self-organizing neural models, *Frontiers in Neuroscience* **16**.
URL: <https://www.frontiersin.org/article/10.3389/fnins.2022.825879>
- Murthy, V. N., Schikorski, T., Stevens, C. F. & Zhu, Y. (2001). Inactivity produces increases in neurotransmitter release and synapse size, *Neuron* **32**(4): 673–682.
URL: <https://www.sciencedirect.com/science/article/pii/S0896627301005001>

- Mäki-Marttunen, T., Iannella, N., Edwards, A. G., Einevoll, G. T. & Blackwell, K. T. (2020). A unified computational model for cortical post-synaptic plasticity, *eLife* **9**: e55714.
- Nadal, J. P., Toulouse, G., Changeux, J. P. & Dehaene, S. (1986). Networks of formal neurons and memory palimpsests, *Europhysics Letters (EPL)* **1**(10): 535–542.
URL: <https://doi.org/10.1209/0295-5075/1/10/008>
- Nair, M. V., Muller, L. K. & Indiveri, G. (2017). A differential memristive synapse circuit for on-line learning in neuromorphic computing systems, *Nano Futures* **1**(3): 035003.
- Neftci, E. O., Augustine, C., Paul, S. & Detorakis, G. (2017). Event-driven random back-propagation: Enabling neuromorphic deep learning machines, *Frontiers in Neuroscience* **11**: 324.
- Neftci, E. O., Mostafa, H. & Zenke, F. (2019). Surrogate gradient learning in spiking neural networks: Bringing the power of gradient-based optimization to spiking neural networks, *IEEE Signal Processing Magazine* **36**(6): 51–63.
- Nelson, S. B., Sjöström, P. J. & Turrigiano, G. G. (2002). Rate and timing in cortical synaptic plasticity, *Philosophical Transactions of the Royal Society of London. Series B: Biological Sciences* **357**(1428): 1851–1857.
- Nessler, B., Pfeiffer, M. & Maass, W. (2009). Sdp enables spiking neurons to detect hidden causes of their inputs, in Y. Bengio, D. Schuurmans, J. Lafferty, C. I. Williams & A. Culotta (eds), *Advances in Neural Information Processing Systems*, Vol. 22, pp. 1357–1365.
- Ngezahayo, A., Schachner, M. & Artola, A. (2000). Synaptic activity modulates the induction of bidirectional synaptic changes in adult mouse hippocampus, *Journal of Neuroscience* **20**(7): 2451–2458.
- Nøkland, A. (2016). Direct feedback alignment provides learning in deep neural networks, in D. Lee, M. Sugiyama, U. Luxburg, I. Guyon & R. Garnett (eds), *Advances in Neural Information Processing Systems*, Vol. 29, Curran Associates, Inc.
- Oja, E. (1982). A simplified neuron model as a principal component analyzer, *Journal of Mathematical Biology* **15**: 267–273.
- Olshausen, B. A. & Field, D. J. (1996). Emergence of simple-cell receptive field properties by learning a sparse code for natural images, *Nature* **381**: 607–609.
- Payeur, A., Guerguiev, J., Zenke, F., Richards, B. A. & Naud, R. (2021). Burst-dependent synaptic plasticity can coordinate learning in hierarchical circuits, *Nature Neuroscience* **24**(1010-1019).
- Payvand, M., Fouda, M. E., Kurdahi, F., Eltawil, A. & Neftci, E. O. (2020). Error-triggered three-factor learning dynamics for crossbar arrays, *2020 2nd IEEE International Conference on Artificial Intelligence Circuits and Systems (AICAS)*.
- Pfister, J. P. & Gerstner, W. (2006). Triplets of spikes in a model of spike timing-dependent plasticity, *The Journal of Neuroscience* **26**(38): 9673–9682.
- Pfister, J. P., Toyozumi, T., Barber, D. & Gerstner, W. (2006). Optimal spike-timing dependent plasticity for precise action potential firing in supervised learning, *Neural Computation* **18**: 1309–1339.
- Querlioz, D., Bichler, O., Dollfus, P. & Gamrat, C. (2013). Immunity to device variations in a spiking neural network with memristive nanodevices, *IEEE Transactions on Nanotechnology* **12**(3): 288–295.
- Rachmuth, G., Shouval, H. Z., Bear, M. F. & Poon, C.-S. (2011). A biophysically-based neuromorphic model of spike rate- and timing-dependent plasticity, *Proceedings of the National Academy of Science* **108**(49): E1266–E1274.
- Ramakrishnan, S., Hasler, P. E. & Gordon, C. (2011). Floating gate synapses with spike-time-dependent plasticity, *IEEE Transactions on Biomedical Circuits and Systems* **5**(3): 244–252.
- Ramón y Cajal, S. (1894). The croonian lecture: La fine structure des centres nerveux, *Proc. R. Soc. Lond., B, Biol. Sci.* **4**, 444–468.
- Rathi, N. & Roy, K. (2021). Sdp based unsupervised multimodal learning with cross-modal processing in spiking neural networks, *IEEE Transactions on Emerging Topics in Computational Intelligence* **5**(1): 143–153.
- Rochester, N., Holland, J., Haibt, L. & Duda, W. (1956). Tests on a cell assembly theory of the action of the brain, using a large digital computer, *IRE Transactions on Information Theory* **2**(3): 80–93.
- Sacramento, J. a., Ponte Costa, R., Bengio, Y. & Senn, W. (2018). Dendritic cortical microcircuits approximate the backpropagation algorithm, in S. Bengio, H. Wallach, H. Larochelle, K. Grauman, N. Cesa-Bianchi & R. Garnett (eds), *Advances in Neural Information Processing Systems*, Vol. 31, Curran Associates, Inc.
URL: <https://proceedings.neurips.cc/paper/2018/file/1dc3a89d0d440ba31729b0ba74b93a33-Paper.pdf>
- Sarpeshkar, R. (1998). Analog versus digital: Extrapolating from electronics to neurobiology, *Neural*

- Computation* **10**(7): 1601–1638.
- Schikorski, T. & Stevens, C. F. (1997). Quantitative ultrastructural analysis of hippocampal excitatory synapses, *Journal of Neuroscience* **17**(15): 5858–5867.
URL: <https://www.jneurosci.org/content/17/15/5858>
- Schmidhuber, J., Wierstra, D., Gagliolo, M. & Gomez, F. (2007). Training recurrent networks by evoluno, *Neural Comput.* **19**(3): 757–779.
- Senn, W., Markram, H. & Tsodyks, M. (2001). An algorithm for modifying neurotransmitter release probability based on pre- and postsynaptic spike timing, *Neural Computation* **13**(1): 35–67.
- Shatz, C. J. (1992). The developing brain., *Sci. Am.* 267, 60–67.
- Sheik, S., Paul, S., Augustine, C. & Cauwenberghs, G. (2016). Membrane-dependent neuromorphic learning rule for unsupervised spike pattern detection, *2016 IEEE Biomedical Circuits and Systems Conference (BioCAS)*, pp. 164–167.
- Sherrington, C. S. (1897). The central nervous system, A Textbook of Physiology, 7th Edn, ed. M. Foster (London: Macmillan), 3, 929.
- Shouval, H. Z., Bear, M. F. & Cooper, L. N. (2002). A unified model of NMDA receptor-dependent bidirectional synaptic plasticity, *Proceedings of the National Academy of Sciences* **99**(16): 10831–10836.
- Sjöström, J. & Gerstner, W. (2010). Spike-timing dependent plasticity, *Scholarpedia* **5**(2): 1362. revision #184913.
- Sjöström, P. J., Turrigiano, G. G. & Nelson, S. B. (2001). Rate, timing, and cooperativity jointly determine cortical synaptic plasticity, *Neuron* **32**(6): 1149–1164.
- Song, S., Miller, K. & Abbot, L. (2000). Competitive Hebbian learning through spike-timing-dependent plasticity, *Nature Neuroscience* **3**(9): 919–926.
- Stuart, G. & Sakmann, B. (1994). Active propagation of somatic action potentials into neocortical pyramidal cell dendrites, *Nature* **367**(6972): 69–72.
- Suárez, L. E., Richards, B. A., Lajoie, G. & Misić, B. (2021). Learning function from structure in neuromorphic networks, *Nature Machine Intelligence* **3**(9): 771–786.
- Tanaka, H., Morie, T. & Aihara, K. (2009). A cmos spiking neural network circuit with symmetric/asymmetric stdp function, *IEICE Transactions on Fundamentals of Electronics, Communications and Computer Sciences* **E92-A**(7): 1690–1698.
- Urbanczik, R. & Senn, W. (2014). Learning by the dendritic prediction of somatic spiking, *Neuron* **81**(3): 521–8.
- Varela, F. J., Rosch, E. & Thompson, E. (1991). *The embodied mind: cognitive science and human experience*, MIT Press Cambridge, Mass.
- Vigueron, A. & Martinet, J. (2020). A critical survey of stdp in spiking neural networks for pattern recognition, *2020 International Joint Conference on Neural Networks (IJCNN)*, pp. 1–9.
- Waldeyer, H. (1891). Ueber einige neuere forschungen im gebiete der anatomie des centralnervensystems, *Dtsch. Med. Wochenschr.* 17, 1352–1356.
- Yger, P. & Harris, K. (2013). The convallis rule for unsupervised learning in cortical networks, *PLoS Computational Biology* **9**(10).
- Zahra, O. & Navarro-Alarcon, D. (2019). A self-organizing network with varying density structure for characterizing sensorimotor transformations in robotic systems, *Towards Autonomous Robotic Systems*, Springer International Publishing, Cham, pp. 167–178.
- Zenke, F. & Ganguli, S. (2018). Superspike: Supervised learning in multilayer spiking neural networks, *Neural Computation* **30**(6): 1514–1541.
- Zenke, F. & Neftci, E. O. (2021). Brain-inspired learning on neuromorphic substrates, *Proceedings of the IEEE* **109**(5): 935–950.
- Ziegler, M., Riggert, C., Hansen, M., Bartsch, T. & Kohlstedt, H. (2015). Memristive hebbian plasticity model: Device requirements for the emulation of hebbian plasticity based on memristive devices, *IEEE Transactions on Biomedical Circuits and Systems* **9**(2): 197–206.
- Lukasz Kuśmierz, Isomura, T. & Toyoizumi, T. (2017). Learning with three factors: modulating hebbian plasticity with errors, *Current Opinion in Neurobiology* **46**: 170–177. Computational Neuroscience.
URL: <https://www.sciencedirect.com/science/article/pii/S0959438817300612>